ABSTRACT

Title of Thesis:	THERMODYNAMICS OF FLUID POLYAMORPHISM
	Lauren Elizabeth Amrhein, Master of Science in Chemical and Biomolecular Engineering, 2017
Thesis Directed By:	Mikhail A. Anisimov, Distinguished University Professor, Department of Chemical and Biomolecular Engineering

"Fluid polyamorphism" is the existence of two alternative amorphous structures in a single-component fluid. It is found in very different materials, such as silicon, phosphorus, cerium, and hydrogen, usually at extreme conditions. In particular, this phenomenon is hypothesized in metastable supercooled water, inaccessible for direct bulk-water experiments because it is predicted to be below the empirical limit of homogeneous ice nucleation. I present a generic phenomenological approach to describe polyamorphism in a single-component fluid, applicable regardless of the microscopic origin of the phenomenon. To specify this approach, I consider a fluid with "chemical reaction" equilibrium between two competing interconvertible states or structures. This approach for the physics of liquid-liquid separation in a single-component fluid is based on a discrete nature of two distinct structures. The approach qualitatively describes the global phase diagram of a fluid, with both vapor-liquid and liquid-liquid equilibria, as well as peculiar properties of polyamorphic fluids.

THERMODYNAMICS OF FLUID POLYAMORPHISM

by

Lauren Elizabeth Amrhein

Thesis submitted to the Faculty of the Graduate School of the
University of Maryland, College Park, in partial fulfillment
of the requirements for the degree of
Master of Science
2017

Advisory Committee:
Professor Mikhail Anisimov, Chair
Professor Jeffery Klauda
Professor Sheryl Ehrman

Dedication

To my support environment: My family, friends, and everyone who helped me work on this research.

Acknowledgements

I would like to acknowledge Dr. Mikhail Anisimov, for working with me throughout this project and for helping me every step of the way. I would like to acknowledge Amanda Rosenbaum for working through so many mathematical and computational problems with me and continuing to support me and be interested in this project. I would like to acknowledge Dr. Michal Duška for helping me with the computational aspects of this project, including with the use of Python for calculations. I would not have been able to finish the project nearly as effectively without his programming expertise. Finally, I would like to acknowledge my family and close friends who supported me throughout this entire project.

Table of Contents

List of Figures

Chapter 1: Introduction

1.1 Fluid Polyamorphism

An interesting phenomenon that can be found in a variety of substances is known as fluid polyamorphism. Similar to solid polymorphism, this phenomena involves the ability of a substance to exist in different structures. However, fluid polyamorphism maintains the same symmetry of polyamorphic states while polymorphism means a change in the symmetry. The idea of polyamorphism has been described since the late 20^{th} century [1]. Polyamorphism is usually described within the liquid region as two distinct phases with disordered structures [2]. Amorphous phases could be different fluids, specifically liquids or supercritical fluids, or glasses. The amorphous structures do not necessarily need to be stable; polyamorphism could exist in the stable and metastable regions of substances [3]. Additionally, amorphous phases may or may not be equilibrium structures. Amorphous structures in liquids are distinguished typically by low versus high density and also a distinct difference in bulk thermodynamic properties [4, 5]. The existence of alternative local structures in fluids may or may not result in phase separation. Should the amorphous structures phase separate, there exists a fluid-fluid phase transition in the particular substance in addition to the common vapor-liquid phase transition.

A lot of experimental and computational (from computer simulations) evidence has pointed to the existence of polyamorphism in many different liquids including: hydrogen, silicon, cerium, phosphorus, triphenyl phosphite, water, and some other molecular substances [6-35]. This phenomena is often accompanied by polymorphic

solid state transitions. The microscopic driving forces for polyamorphism in different substances may be fundamentally different.

For example, the driving force for polyamorphism in cerium is thought to be a consequence of the delocalization of Fermi orbital electrons as well as the interactions between Fermi orbitals themselves [6]. Cerium has a rich phase diagram with polymorphism as well as the simulated liquid-liquid transition. Recent studies have shown evidence of a liquid-liquid transition in cerium at high temperature and high pressure that is believed to terminate at a critical point [6]. The study of cerium combined X-ray diffraction studies with *ab initio* simulations. Figure 1 below shows the predicted phase diagram of Cerium, with solid polymorphism appearing to influence the liquid polyamorphism at higher temperatures and pressures.

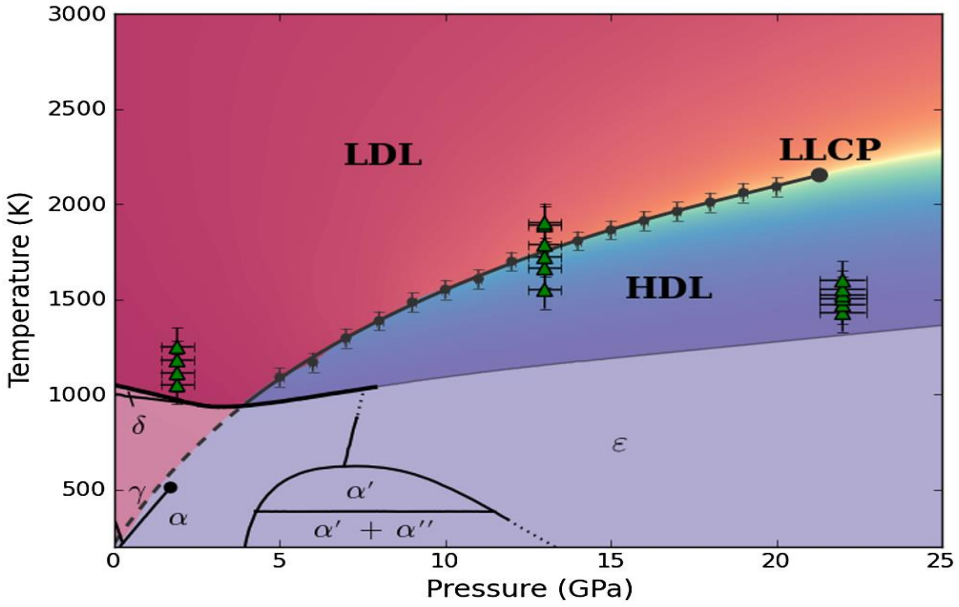

Figure 1. Reproduced from [6]. Phase diagram of cerium overlaid with experimental data. Green triangles indicate experimentally observed liquids. The liquid-liquid transition line is denoted by the gray points and lines determined by *ab initio* simulations. Greek symbols indicate various solid polymorphs.

The driving force for polyamorphism in phosphorus is a transition between a polymeric liquid and a monomeric liquid [7-9]. Recent experimental studies have produced evidence showing that a known liquid state of phosphorus can be transitioned to a polymeric, viscous liquid. This transition is pressure-induced and reversible, meaning that the transition back to the known form of liquid phosphorus happens by simply changing the pressure [7-9].

Phosphorus' polyamorphism is similar to a transition from non-metallic hydrogen to metallic hydrogen [10]. The transition takes place at extremely high pressures—between 120 GPa and 140 GPa at temperatures between 500-2000 K [11]. Evidence from high pressure Raman spectroscopy studies has also reported a transition at pressures higher 325 GPa at 300 K [12]. Molecular hydrogen makes a transition from an insulating non-conductive phase to a metallic, dense and conductive phase [13]. Morales et al. [14] have found evidence of hydrogen's polyamorphism in quantum simulations. The critical point predicted from the simulations was at 2000 K and 120 GPa [14]. This transition is an association and dissociation reaction in which the hydrogen would transform from atomic hydrogen to molecular hydrogen [13]. An important feature of the liquid-liquid phase transition is the existence of a maximum of the thermodynamic response functions that will all converge on the critical isochore. Li et al. [15] present evidence of the existence of the Widom line for supercritical hydrogen. This liquid-liquid transition appears in the supercritical region of the hydrogen phase diagram with respect to the vapor-liquid transition at extremely high pressures and temperatures. Figure 2 shows the hydrogen phase diagram along with the fluid-fluid transition line.

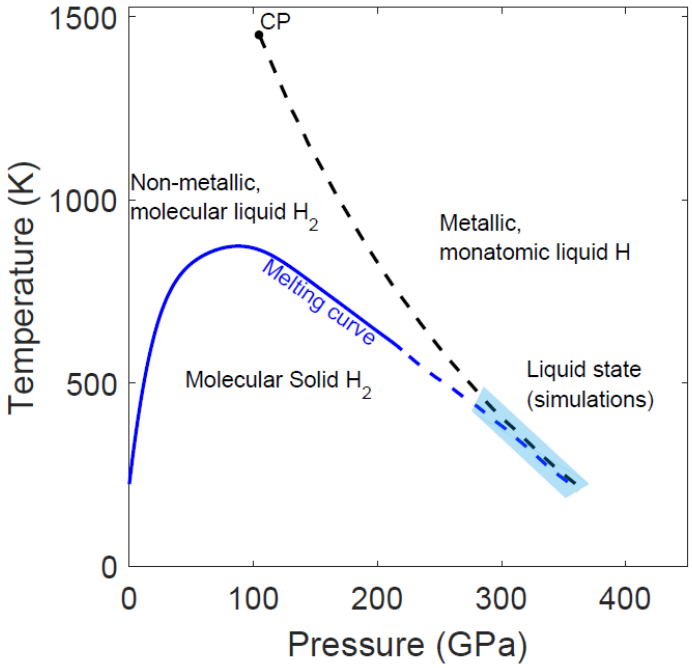

Figure 2. Potential phase diagram for hydrogen showing the solid polymorphs, the melting line, and the potential liquid-liquid phase transition line in supercritical hydrogen.

Triphenyl phosphite's liquid-liquid transition is thought to occur near the temperature of the stability limit of the liquid [2,16]. This transformation is to a very viscous state, called the glacial phase. Bulk experimental studies of triphenyl phosphite have determined that quenching of the fluid will result in a transformation to a very viscous amorphous state [2]. The glacial phase has its own glass transition temperature separate from the glass transition temperature of the original liquid triphenyl phosphite phase, further determining its stability as a new amorphous phase [2,16].

Silicon's tetrahedral structure is thought to be a major factor in its polyamorphism [17-27]. Silicon, as well as other network-forming liquids, like water, has a tendency to form local structures with tetrahedral molecular geometry. This means that the average coordination number of these open local structures is around four. This ability

of silicon and other network-forming liquids to form tetrahedral open structures is thought to be the main driving force of liquid-liquid transitions between phases with different coordination numbers [18]. The predicted phase diagram of silicon from MD simulations is shown in figure 3. The MD simulations by the authors in [18] has predicted that liquid-liquid critical point in silicon will be in the negative pressure region—a doubly metastable region. A doubly metastable state means that this silicon is both supercooled and superstretched, being metastable with respect to both solid and vapor.

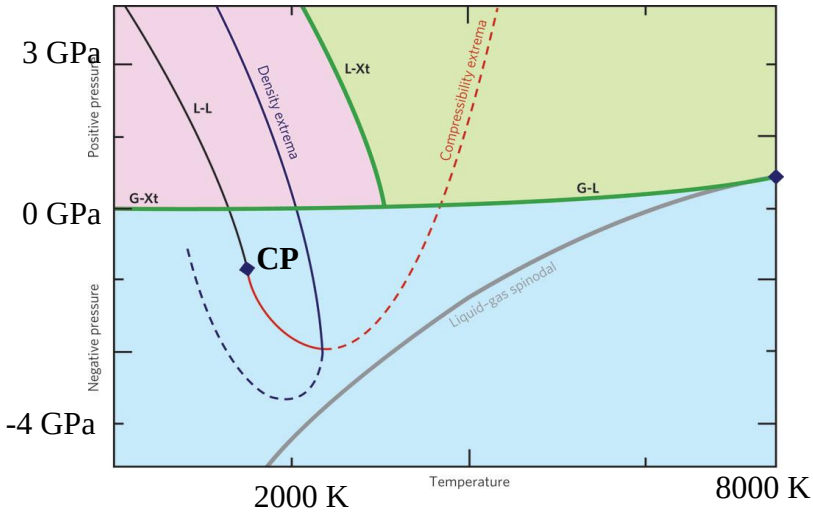

Figure 3. Adapted from [18]. Proposed phase diagram of silicon depicting the vapor-liquid transition line (G-L), the liquid-crystal melting line (L-Xt), the vapor-crystal transition line (G-Xt), the vapor-liquid spinodal, and the proposed liquid-liquid transition line (L-L). Density and compressibility extrema lines are shown in blue and red, respectively. The liquid-liquid transition line terminates at a critical point proposed by [26] with the value T_c~1120 K, P_c~ -0.60 GPa.

Silica, SiO_2, is another liquid, similar to water, that is predicted to exhibit polyamorphism. The authors in Refs. [28-32] report results of molecular dynamics simulations that show an amorphous-amorphous transition in silica at high pressures. However, silica has currently no known critical point in the available simulations. Lascaris et al. [32] search for the critical point using two separate models of silica at

lower temperatures than most simulations for silica. They found that there is no liquid-liquid critical point in any of the models and simulations that currently have found a transition in silica. They were unable to find an exact critical point, but found that there is behavior that appears to be close to the critical behavior at 4000 K and 5 GPa [32].

Carbon is a material with well-known polymorphs in graphite and diamond. However, carbon also has been found to exhibit liquid polyamorphism. Glosli and Ree [33] present simulation results that show a liquid-liquid phase transition in liquid carbon. Carbon's liquid-liquid transition takes place in thermodynamically stable fluids; this is different from liquids like silicon, where the liquid-liquid transition is in a metastable region of the phase diagram. Glosli and Ree find that carbon has a liquid-liquid critical point at 8801 K and 10.56 GPa [33]. The main difference between the distinct two liquid carbon states is hypothesized to be a change in the hybridization of carbon orbitals [33]. Yttria-Alumina melts may also have liquid polyamorphism. Refs. [34-35] report conflicting experimental evidence of a liquid-liquid phase transition in yttria-alumina. Ref. [34] determines that there is a liquid-liquid phase transition based on X-ray diffraction experiments. However, authors of ref [35] believe that there is no evidence for a structural transition in yttria-alumina melts based on their experiments on the time of crystallization.

One very important point to note from all of the different liquids exhibiting polyamorphism is that much of the polyamorphism happens at extreme conditions. Many of these fluids can be either supercritical fluids, supercooled liquids, or stretched liquids (when a liquid is taken to negative pressures). Also, fluid polyamorphism is difficult to observe experimentally due to the extreme conditions. As a result, much of

polyamorphism is observed through simulations. However, simulation results may also be ambiguous and difficult to interpret because of finite size effects and long equilibration times [82].

A final intriguing aspect of the phenomenon of polyamorphism is the connection between dynamics and thermodynamics [37]. Polyamorphic liquids often exhibit a transition from a strong liquid to a fragile liquid [36-40]. Strong liquids are structurally sound and the structure of the liquids often stays constant over ranges of temperature. Strong liquids will change to fragile liquids through a change in the density. Fragile liquids are of a lower density with a structure that is not as stable as strong liquids and may change easily with temperature [36]. This transition is a dynamic change in the viscosity of the liquid. Typically strong liquids exhibit Arrhenius behavior over temperature, while fragile liquids exhibit very non-Arrhenius behavior [40]. Figure 4 shows the behavior of a potentially polyamorphic liquid, water, in a fragile to strong transition.

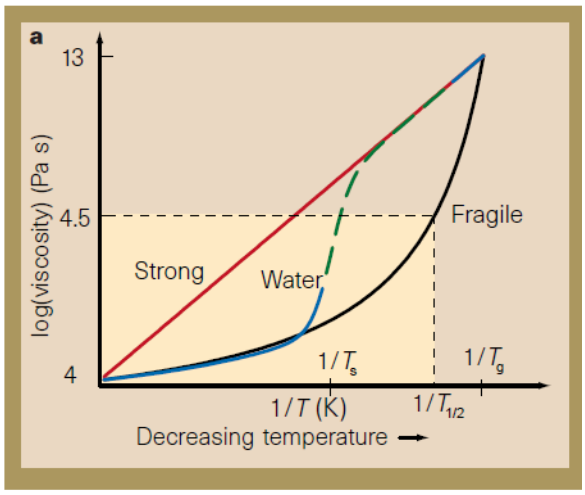

Figure 4. Reproduced from [38]. Viscosity of liquids as a function of inverse temperature. The viscosity of strong liquids increases linearly while that of fragile liquids increases non-linearly. Water exhibits a fragile to strong transition, at T_s, before it reaches the glass transition temperature T_g. $T_{1/2}$ is where $\log(\eta(T)) = \frac{1}{2} \log(\eta(T))$.

1.2 Water as a Polyamorphic Fluid

Water is a liquid of particular interest due to its wide variety of uses in industrial applications. Water specifically is one of the most abundant substances on Earth [42]. Since the 1980s, a large number of experiments have been done on cold, supercooled, and glassy water, attempting to understand more about some of the anomalous properties in water [41]. Additionally, the polyamorphism hypothesized in water is thought to be similar to a variety of tetrahedral network forming liquids [3]. Several anomalies that are present in water are also present in other tetrahedral network forming liquids. The presence and interaction of these anomalies are thought to be a product of a liquid-liquid phase transition. For example water exhibits a density maximum at 4 degrees Celsius [48]. In some models to describe water, the density anomaly necessarily means that there will be a liquid-liquid phase transition [109]. Additionally, heat capacity and compressibility, the thermodynamic response functions, increase upon supercooling and reach apparent maximums in the metastable region [48]. The thermal conductivity also reaches a minimum at the same time the heat capacity reaches a maximum [44]. A variety of research has been done on the behavior of the density and the response functions—some of which is shown in Refs [43-50,64]. The apparent anomalies in the thermodynamic response functions has created a large area of research in supercooled water.

The researchers in this field have looked to identify the cause of these anomalies in supercooled water. A popular theory is the idea of a liquid-liquid phase transition—fluid polyamorphism—in deeply supercooled water that is just below the reach of bulk experiments, due to the homogeneous ice nucleation that happens at 232 K [48]. Figure

5 shows a possible phase diagram for water, proposed by Poole et al. [49]. The brown curve denotes the coexistence which is terminated by a critical point, proposed by Holten and Anisimov [65].

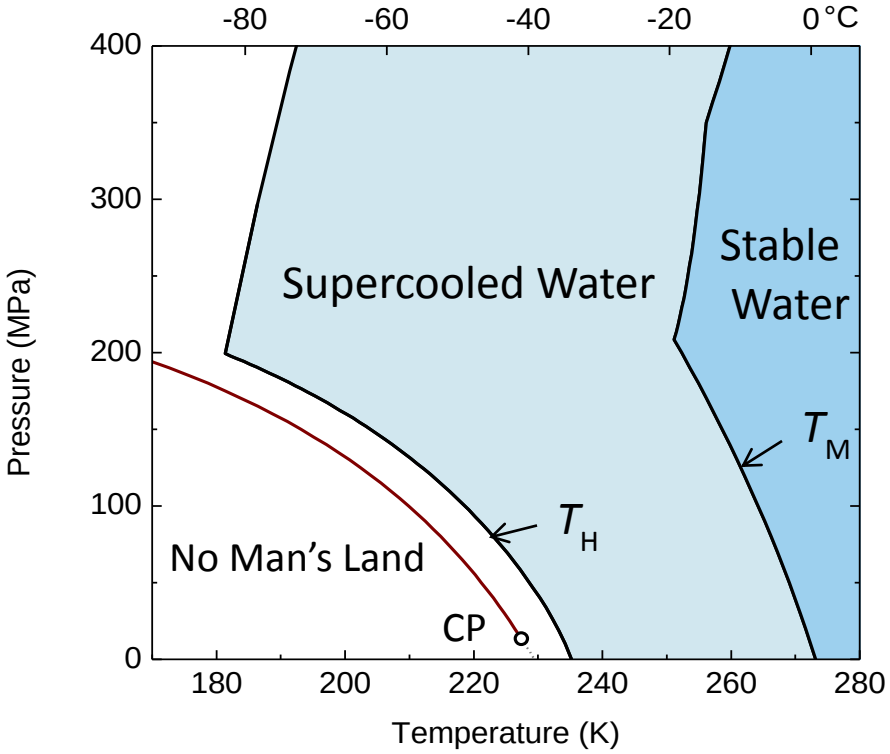

Figure 5. Proposed phase diagram for water adapted from [49]. T_H denotes the line of homogeneous ice nucleation. T_M denotes the melting line, splitting stable water from supercooled water. The brown line is the proposed coexistence line between HDL and LDL. It is terminated by a possible critical point proposed by [65].

There are four scenarios that are proposed to explain the anomalous behavior of water. The first scenario is the existence of a liquid-liquid transition in water that terminates at a critical point [48]. The second scenario is the "critical point free" scenario. It hypothesizes the existence of a liquid-liquid transition, except the critical point is exactly at or below the limit of stability, making the transition first order in the entire stable and metastable region [48]. The third scenario is the "singularity-free scenario," where the critical point is exactly at 0 K and no physical liquid-liquid

transition exists [48,52]. The fourth scenario ("retracing spinodal scenario") depicts the possibility that the liquid-vapor spinodal (the limit of stability of the liquid state with respect to vapor) actually retraces and reenters the phase diagram at positive pressures. This reentrance is what causes the anomalies in water [48,53]. The "retracing spinodal" scenario was criticized in the literature because it suggests that the spinodal would cross the metastable vapor-liquid transition, which in turn would require the existence of an additional vapor-liquid critical point below the melting temperature [Debenedetti].

In this thesis I have shown how the first three scenarios can be explained by the same thermodynamic model. The most probable and most studied scenario is scenario one—a liquid-liquid transition that terminates at a critical point in the positive pressure region. There is a rich history of the study of water's polyamorphism, gaining popularity in the 20th century. Recently, there has been a variety of computational studies in models of water to study water's possible polyamorphism in Refs [57-61,63,65-85,116-118]. There are several popular atomistic models of water studied by simulations such as ST2, TIP4P/2005, mW, etc. None of these models perfectly describe all properties of water. In 1992, Poole, Sciortino, Essman, and Stanley found a liquid-liquid transition in the ST2 model of water. These authors found a first order phase transition, with a critical temperature around 235 K and a critical pressure at 200 MPa [67]. Many other simulations have predicted a positive critical point in water, but a few have predicted that the critical point will lie in negative pressures [48]. Additionally, some models do predict a liquid-liquid transition in supercooled water, while other models do not predict a transition at all.

Holten et al. [66] examined the ST2 model for phase behavior through utilizing a two state model equation of state. They showed thermodynamic behavior that supported the information previously published by Poole et al. [49,67]. Figure 6 shows the information on the liquid-liquid phase transition, as well as the extrema lines for density, heat capacity and compressibility determined by Poole et al. [67].

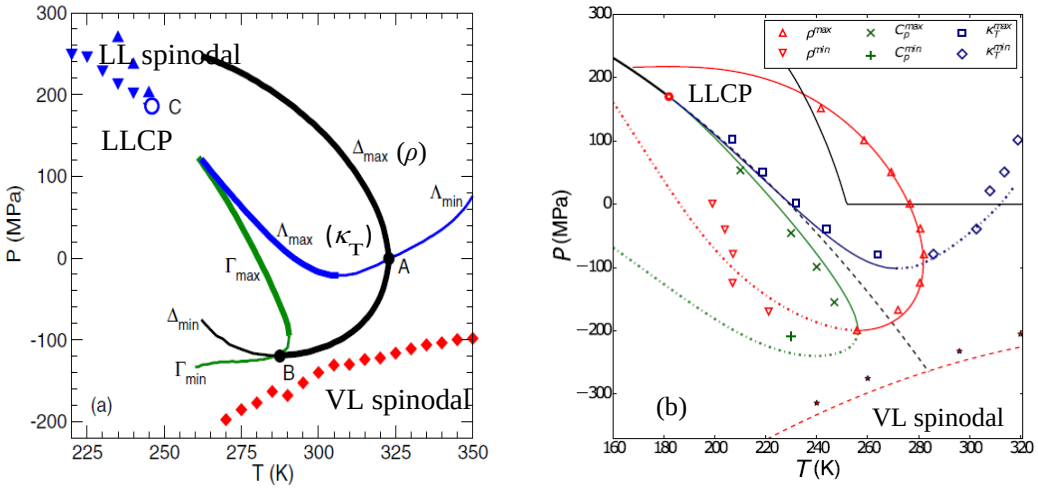

Figure 6. (a) Adapted from [67]. Simulations of the ST2 model of water depicting a liquid-liquid transition with a liquid-liquid critical point. Shown with extrema lines of density (black, $\Delta_{max}/\Delta_{min}$), compressibility (blue, $\Lambda_{max}/\Lambda_{min}$), and heat capacity (green, $\Gamma_{max}/\Gamma_{min}$) along with the vapor-liquid spinodal (red dots). (b) Adapted from [72]. Simulations of the TIP4P/2005 model of water depicting a liquid-liquid transition with a liquid-liquid critical point. Shown with extrema lines of density (red triangles/ line), compressibility (blue squares/line), and heat capacity (green crosses/line) along with the vapor-liquid spinodal (red dotted line).

The model using the two structure equation of state (TSEOS) was able to describe a liquid-liquid phase transition and the fraction of each state as computed in the simulations. Additionally, the model with the two structure equation of state (TSEOS) shows the increase and divergence of thermodynamic response functions that are indicative of a phase transition [66]. Equation of state by Holten et al. [127] was used

as the international guideline for supercooled water issued by the International Association for the Properties of Water and Steam in 2015.

The TIP4P/2005 model was originally created and described by Abascal and Vega [51]. Singh et al. [69] examined the TIP4P/2005 model of water for phase behavior using a two-structure equation of state. They discovered that the TIP4P/2005 model of water does exhibit a liquid-liquid phase transition in the supercooled region. By fitting the two-structure equation of state to previous simulation results, as well as completing some new simulation results, Singh et al. was able to adequately mimic the anomalous properties of water exhibited by the TIP4P/2005 model [69]. This model of water does exhibit a liquid-liquid transition in supercooled water, as well as the maximum of density and increasing response functions [69]. Figure 5b shows the phase diagram and extrema lines of the response functions in the TIP4P/2005 model of water [72].

However, liquid-liquid separation are not demonstrated by all atomistic models of water. Holten et al. [68] examined the mW model of water for phase behavior utilizing a two-structure equation of state. This model of water did not exhibit a phase transition, meaning that the nonideality of the mixture of two states was not strong enough to induce phase separation [68]. The mW model and the two-structure equation of state are able to predict anomalous properties of supercooled water, such as the maximum of density and increase of heat capacity and compressibility upon supercooling [68]. The mW model does not, however, predict a liquid-liquid transition, meaning that the nonideality is enough to overcome the ideal Gibbs energy of mixing [68].

Because of the line of homogeneous ice nucleation, there is no direct way to observe a metastable liquid-liquid transition in water. As seen above, there are a variety of

models of water that may or may not predict a liquid-liquid transition. However, within the liquid-liquid transition itself, there is a question of where a critical point would be, if there would be a critical point at all. Fuentevilla and Anisimov [55] use a scaled parametric equation of state to predict the location of the critical point and found that based on their equation of state, the critical point would be lower than in most simulations. The position of the critical point is still a major question in the study of water's polyamorphism, due to the large range of possible critical points.

Mishima has most elegantly predicted a possible liquid-liquid critical point [48]. Mishima studied the melting of high pressure ice within the region of stability of hexagonal ice. He ensured that he did not miss the liquid phase when changing temperature and pressure in his system by using water emulsions in oil [48]. The most important finding from this work was the discovery of a kink in the melting lines of ice IV and V— two of the many polymorphs of water. This kink was based on a 20% basis between a high density liquid water and a low density liquid water. Mishima determined that this kink happened on the melting lines of ices IV and V, but this kink did not exist along the melting line of ice III [48]. If Mishima's analysis is correct, and is believed to be correct, this would pin the critical point down to the region between the melting lines of ice IV and ice III. The critical point would be between 0.02 and 0.07 GPa (critical pressure) and between 223 and 230 K, confirming the positive pressure critical point scenario [48]. However, there are some doubts that Mishima was actually observing water and not the transition to the stable hexagonal ice [48]. These doubts do not allow for ruling out a negative pressure critical point for water's polyamorphism.

Holten et al. [85] utilized currently available experimental data to optimize the possible location of a liquid-liquid critical point. Experimental data up to 400 MPa was considered and they found that the location of the critical point proved to be extremely uncertain. There is a wide range of temperature and pressures possible for the location of the liquid-liquid critical point in the supercooled region of water [85]. Figure 7 shows the optimization of the critical point using both an asymptotic model and an extended model. The models use different sets of experimental data to determine the optimal critical point area, with the extended model using the data up to 400 MPa pressure [85].

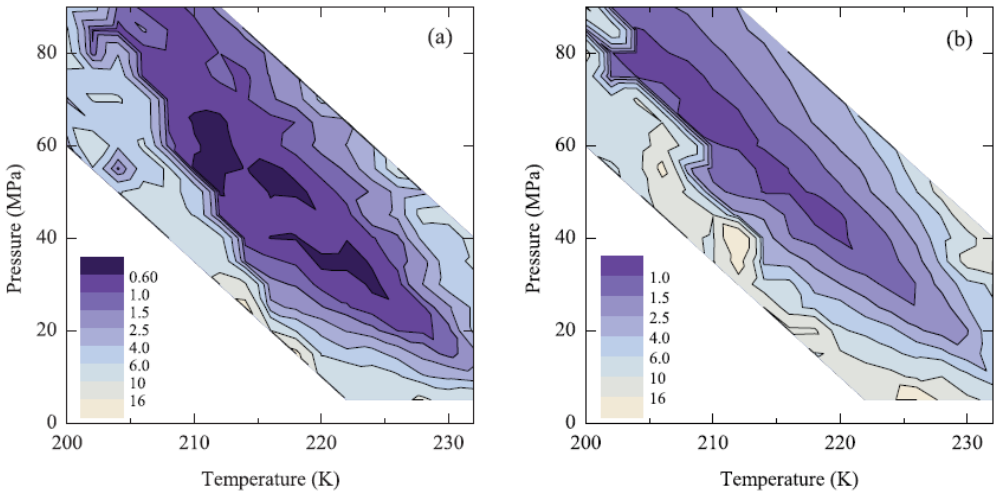

Figure 7. Reproduced from [85]. (a) The asymptotic model using a smaller range of pressure data. (b) The extended model using experimental data up to 400 MPa.

A result of the debate about where a possible liquid-liquid critical point in water would be is a large interest in research on the topic. An increase in research has led to a variety of computational methods to be created and used, including a large number of simulations. Additionally, experimental data in low temperature water has also increased in number due to the interest in this particular anomaly of water. Many of these groups involved in the research has taken a large variety of approaches to

modeling water's polyamorphism. The scope of polyamorphism crosses so many different substances that it is useful to look to model the phenomenon with a generic approach such that many different systems could be described well.

1.3 Two State Thermodynamics

The idea that single component fluids could be described by a model using two alternative states goes back to the 19th century. The idea of two states competing in a single component fluid was first introduced by Whiting [86]. Later, Rontgen [87] also discussed two states, specifically in cold liquid water. The assumption was that supercooled liquid water could exist as water particles and ice particles. However this assumption is now proved incorrect. Water can be described as a mixture of two different locally favored structures—a high density (water like) structure, and a low density (ice like) structure. The ideas of Whiting and Rontgen essentially explain a two structure mixture of a low energy/low entropy state and a high energy/high entropy state. Tanaka [54] described a model using the idea of two states with respect to density order and bond ordering to model liquid water. Mishima and Stanley [62] also discussed generally that water could exist along two different characteristic length scales. The models simplify the complexity of water to just a mixture of the two separate structures.

Recently, there have been other approaches to modeling polyamorphic systems using other two state model approaches. Refs [88-96,111-114,119] all discuss theoretical models of two states of water and whether or not these two states could be stable or unmix. Tanaka [48] has determined that low entropy locally favored structures

can form within a sea of higher entropy normal liquid structures. Two states can be modeled phenomenologically by a bimodal distribution of local molecular structures or configurations and defines cold or supercooled water as a "mixture" of these two specific states. A specific fraction of both of these states can be controlled by changing pressure and temperature. Bertrand and Anisimov [56] used a two state concept to describe a lattice-gas, a focus that typically describes vapor-liquid transitions, and a lattice liquid, a formulation similar to a lattice gas that will exhibit an entropy driven phase separation. Anisimov and colleagues [48] described an ideal entropy of mixing between two structures in competition with a nonideal part of the Gibbs energy of mixing.

This formulation has three major outcomes. First, if the solution of two states is ideal, the liquid will remain homogeneous for all temperatures and pressures. The existence and mixing of two states is not an assumption that the liquid will phase separate [48]. However, the competition between the two states could be the cause of the density maxima and other anomalies in the thermodynamic response functions [48]. A nonideal mixture of two states could result in a positive excess Gibbs energy. If the positive excess Gibbs energy is large enough, it could overcome the entropy of mixing and cause phase separation into two liquid phases. Otherwise, if the excess Gibbs energy is not enough to overcome the entropy of mixing, the solution will be nonideal but will not separate [48]. Excess Gibbs energy could be associated with either the enthalpy of mixing or the excess entropy. The separation would be energy driven if the excess Gibbs energy comes from the enthalpy of mixing. The separation will be entropy driven if the excess Gibbs energy comes from the excess entropy [48].

These local structures are most likely different coordinations of hydrogen bonds. The high density structure would be similar to a tetrahedral formation with water relatively closely packed. The low density structure would be an open structure where the water has a lower coordination number. Henceforth in this paper the high density structure of water will be known as HDL and the low density structure will be known as LDL. The interaction of these locally formed configurations and hydrogen bonding networks gives rise to a pseudobinary behavior in water. The researchers in Refs. [97-108,110] performed experiments attempting to determine that there are two distinct local structures that can be found in supercooled water.

Small angle x-ray scattering has been employed to observe supercooled water. Recent experiments [48] observed inhomogeneities in the density of the liquid that increased upon more cooling. This experiment was interpreted to corroborate the two state claim, with support from a statistical mechanics perspective [48]. X-ray absorption spectroscopy has found evidence of two local structures in water as well. The structures are either very tetrahedral or very disordered. There are two absorption peaks that are interpreted as either a distorted hydrogen bond—corresponding to the disordered water—or as a strong hydrogen bond—corresponding to the tetrahedral formation [48]. The most convincing evidence for two local structures of water comes from x-ray emission spectroscopy. These studies have revealed that there are two sharp peaks in water that may interconvert but do not broaden with increasing temperature [48]. The two peaks can be attributed to both the HDL and LDL.

Evidence of two structures has been found by Taschin et al. [97]. Taschin et al. claim that through an investigation of vibrational dynamics and the process of

relaxation in supercooled water they are able to observe evidence of two coexisting structural configurations. The structures found in this study are thought to be the local structures associated with HDL and LDL. Figure 8 shows the vibrational data at different temperatures discovered by Taschin et al. [97].

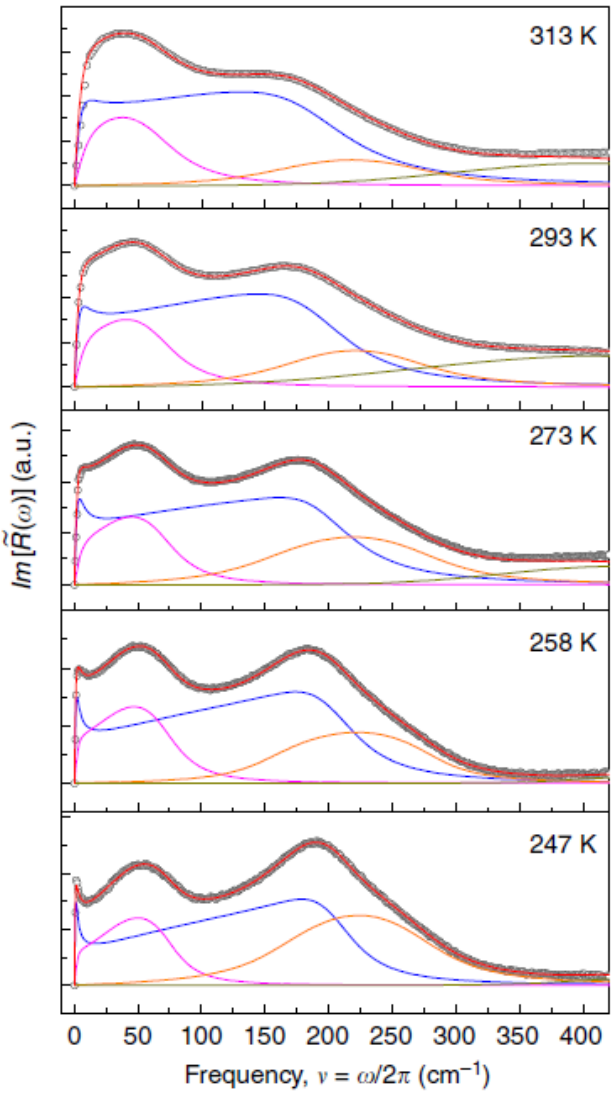

Figure 8. Reproduced from [97]. The imaginary part of the Fourier transform of the time resolved optical Kerr effect data is plotted versus the frequency of light for a variety of temperatures. The red line/open circles are the raw data. The three curves (blue, magenta, orange) are the de-convoluted waves. Orange and magenta lines correspond to the two structures interpreted by [97]. Blue curve is the background data found.

There is a clear development of two separate frequency peaks from the time resolved optical Kerr effect experiments of Taschin et al. As the temperature is lowered, a high frequency peak begins to grow and becomes more pronounced compared to a shorter frequency peak in the data, clearly corresponding to two separate time scales. Taschin et al. [97] interpreted this data as evidence for two different structures in water. Recently, Sellberg and coworkers [98] claim to have probed the structure of water below the temperature of homogeneous ice nucleation. This group used X-ray probing on the order of femtoseconds to determine that there are two distinct local structures of supercooled liquid water below the ice nucleation temperature, but before freezing [98]. In addition to bulk experiments of dynamics, the study of molecular dynamics simulations has also found evidence of two structures of water. Figure 9 shows the two length scale distribution found in the TIP4P/2005 model for water. The combination of information from both experiments and simulations support the idea of two distinct local structures in cold and supercooled water.

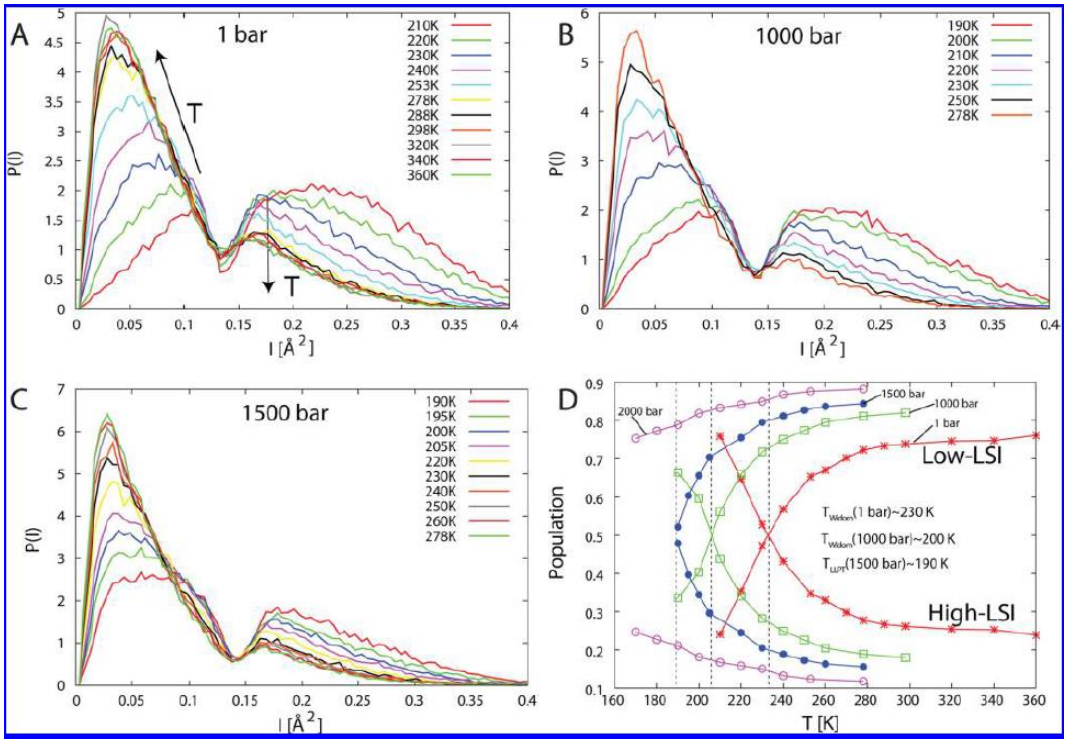

Figure 9. Reproduced from [48]. (a) Local structure index (LSI) analysis of 1 bar pressure in the TIP4P/2005 model showing two length scales and their frequency at different temperatures. (b) LSI analysis of 1000 bar pressure in the TIP4P/2005 model showing two length scales and their frequency at different temperatures. (c) LSI analysis of 1500 bar pressure in the TIP4P/2005 model showing two length scales and their frequency at different temperatures. (d) Fraction of molecules in each distribution as a function of temperature, shown for the three different pressures.

1.4 Approaches to Modeling Polyamorphism

Scientists have taken different approaches when modeling polyamorphism, while trying to correctly create the patterns of the anomalies found in supercooled liquid water. Some of these approaches are easily reconcilable and can be physically explained to be similar to other approaches. However, most of these approaches are specific for water or the fluid in question. For scientific simplicity, it is useful to determine a generic approach to polyamorphism that could work for a variety of different fluids and still capture the anomalies present in different fluids. Approaches

of special interest include the double well potential approach, the hydrogen bond strength approach, and multiple lattice gas approaches.

The double well potential approach to modeling a fluid's polyamorphism is based on a ramp two scale potential and a Lennard-Jones potential. In this approach, a second minimum is added to the well potential that allows for the creation of a second critical point, corresponding to a liquid-liquid transition. A generic soft core double well potential indicates two characteristic length scales for the system being modeled. The two length scales correspond to a hard repulsion sphere and a soft repulsion area. The two length scales also allow the system to exhibit two critical points, corresponding to a vapor-liquid critical point and a liquid-liquid critical point, respectively. Specific potentials have been studied to model fluid behavior in refs [120-123].

The most popular form of potential used for the study of liquid polyamorphism is the Jagla-like potential, a potential characterized by a hard core repulsion scale, followed by a soft (with a linear ramp) repulsive potential and a ramp of attraction at longer distances. A typical Lennard-Jones potential does not exhibit both a vapor-liquid and liquid-liquid transition in a fluid, whereas the Jagla potential is the simplest model that exhibits both transitions. The model creates a liquid-liquid transition in simulations [120]. Figure 10 shows a typical Jagla potential with an attractive ramp used by Buldyrev et al. [120]. This potential is spherically symmetric and is able to qualitatively reproduce some anomalies in waterlike fluids, and most importantly, demonstrates a liquid-liquid transition in simulations [120].

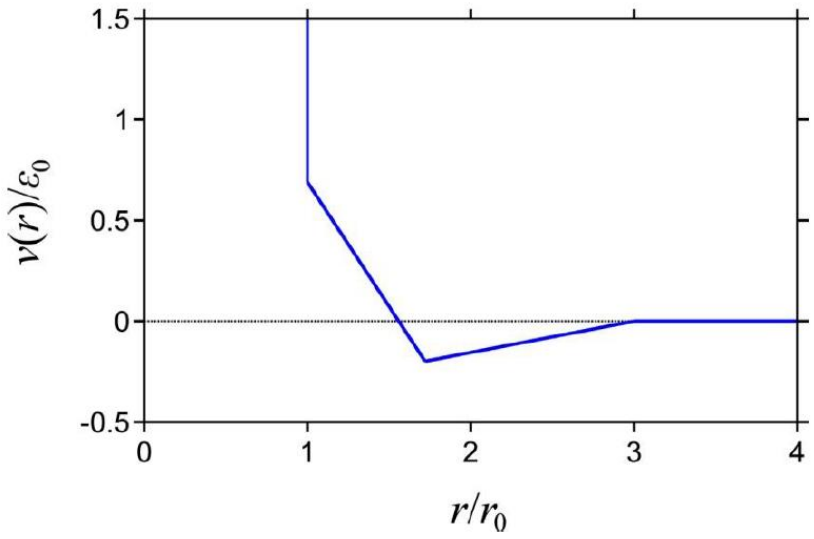

Figure 10. A standard two-scale Jagla potential of energy $v(r)/\varepsilon_o$, nondimensionalized by energy ε_o versus the distance r scaled by a repulsion distance r_o. Reproduced with permission from Ricci and Debenedetti [134, to be published]

Buldyrev et al. [120] have reviewed the work of double well interatomic pair potentials and their relevance to polyamorphism. Specifically, the authors discuss the benefits of using a Jagla potential to model polyamorphism. They discussed that Jagla potentials are very good at modeling both a vapor-liquid critical point and a liquid-liquid critical point [120]. The Jagla potential can also model the specific anomalies that are present in supercooled water and other similar fluids. One problem with the Jagla model in terms of practicality is the slope of the liquid-liquid transition line [120]. The liquid-liquid transition line in the Jagla potential has a positive slope, as opposed to most simulations that model polyamorphic fluids, which suggest that the liquid-liquid transition line has a negative slope [120]. Other than this single drawback, the Jagla potential models the hypothesized polyamorphism and anomalies of supercooled water very well.

In the hydrogen bond strength approach, a specific energy in the form of a Hamiltonian is attributed to the thermodynamics of water, with an added energy to simulate the nonideality in the fluid. This energy form allows for the anomalies shown in water to be similar to those observed experimentally [129]. Stokely et al. [129] have used this approach to model water to allow for every possible scenario of critical point. They defined the strength of hydrogen bonds as an energy difference between different types of hydrogen bonds as one parameter. Their second parameter is the cooperativity of hydrogen bonds, defined as whether hydrogen bonds form independently of other molecules (limit as cooperativity reaches zero) or the hydrogen bonds form because of and due to the other molecules and hydrogen bonds (limit as cooperativity becomes large) [129]. This formulation of parameters is able to mimic the anomalies of water as well as create all four possible scenarios of the position of the liquid-liquid critical point in water. Figure 11 shows the relationship between the two parameters that Stokely et al. [129] defined. The figure also describes which scenario each combination of parameters will create.

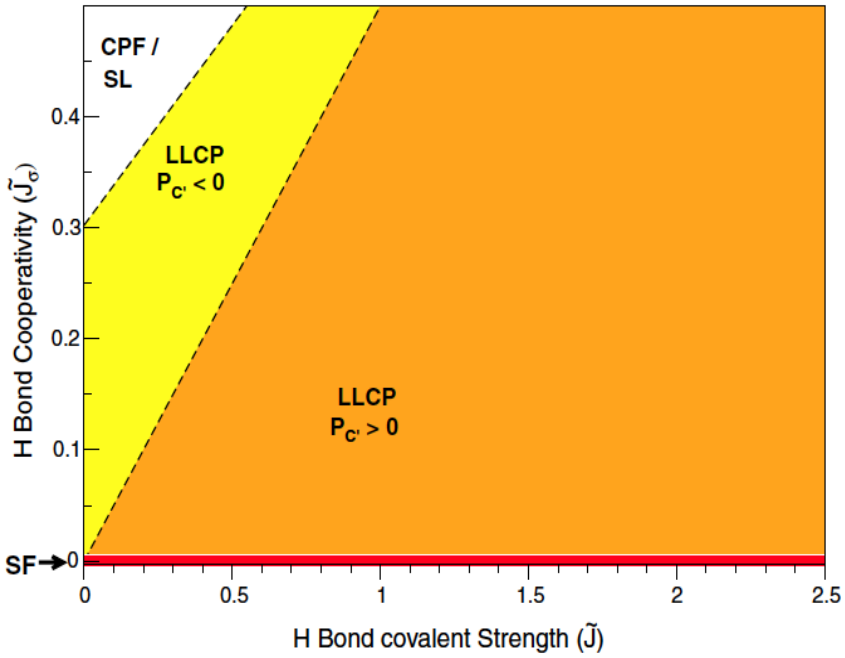

Figure 11. Reproduced from [129]. A plot of hydrogen bond cooperativity versus the hydrogen bond covalent strength. Orange denotes the critical pressure of the liquid-liquid transition is larger than zero. Yellow denotes that the critical pressure is less than zero. White denotes that the critical pressure is below the vapor-liquid spinodal. The red line at cooperativity equals zero is the ideal solution case.

Ciach and colleagues [130] utilized a statistical mechanics approach to determine the possible behavior of supercooled water. They use a lattice gas approach with cells of ordered water, disordered water, and empty cells. The purpose of this study was to create a model that would predict the properties of water including anomalies. Specifically in the study, "water is treated as a mixture of two components, whose chemical potentials are *not* independent" [130]. The model was found to predict the properties of water well on a qualitative level in the mean-field approximation. The shapes and response functions that Ciach and colleagues determined from their model is in good agreement with the shape of previous theoretical and experimental results [130].

Poole et al. [131] took an approach similar to both Stokely et al. and Ciach et al. in describing the properties of water. Using the van der Waals equation of state, this group defined a Helmholtz free energy that accounted for contributions from the original van der Waals interactions and also an added Helmholtz energy of hydrogen bonds, which takes into account the fraction of molecules that will create the strong hydrogen bonds associated with water's tetrahedral local structure [131]. Poole et al. used this model to calculate the phase diagram and coexistence of water. They were able to investigate the positive pressure critical point scenario and the reentrance of the spinodal scenario. The model qualitatively matched the patterns of water's behavior and anomalies [131].

1.5 Goals and Motivation

Modeling polyamorphism has had a rich history in research. From sophisticated interatomic potentials to discrete lattice gas models, polyamorphism is often described specifically to the system. It is useful for the research of liquid polyamorphism to develop a simple approach to model a variety of systems. The question arises: what is fundamentally common in all, physically very different fluid systems exhibiting polyamorphism? In this paper, I present a generic phenomenological approach to describe fluid polyamorphism in a single-component substance, which is applicable regardless of the difference in microscopic nature of the phenomenon. To specify this approach and calculate thermodynamic properties, I consider a fluid with "chemical reaction" equilibrium between two competing interconvertible molecular structures.

The idea to consider two interconvertible states to describe liquid polyamorphism is not new. However, in all previous studies, the liquid-liquid transition was considered as being independent of the vapor-liquid transition in the same substance. In other words, one of the alternative states (which is responsible for vapor-liquid transition) was described simply empirically. In the novel approach, I propose a simple equation of state which generically describes both liquid-gas and liquid-liquid transitions in the same single-component fluid. This approach for the physics of liquid-liquid separation in a single-component fluid is a discrete approach driven by the existence of two distinct interconvertible structures. The approach qualitatively describes the global phase diagram of a fluid, with both vapor-liquid and liquid-liquid equilibria, as well as the peculiar properties of polyamorphic fluids.

Chapter 2: Methodology

2.1 General Formulation of Polyamorphism

A generic thermodynamic description of fluid polyamorphism can be formulated in the framework of Landau theory of phase transitions, in which the concept of the order parameter plays the key role [132]. The Gibbs energy (per molecule) *G* of a single-component fluid can be generally presented in the form

$$G(p,T,\phi) = G_0(p,T) + kTf(\phi) - h\phi, \qquad (1)$$

where *p* is the pressure, *T* is the temperature, *k* is Boltzmann's constant, ϕ is the "order parameter" (an additional scalar variable that characterizes an alternative amorphous structure), $h = h(T, p)$ is a thermodynamic field conjugate to the order parameter (known as the "ordering field"), $f(\phi)$ is a function which specific form depends on the microscopic nature of the order parameter. One must note that Eq. (1) is applicable to different phenomena and systems with different physical nature of the order parameter and, correspondingly, of the ordering field. However, while, for example, in the application to magnetization, *h* is the magnetic field that is an independent variable, in polyamorphic fluids the ordering field is a function of pressure and temperature. I also note that the ordinary gas-liquid transition is originally described by the part of the Gibbs energy independent of ϕ, $G_0(p,T)$.

The equilibrium value of the order parameter is found by minimizing the Gibbs energy as $(\partial G/\partial\phi)_{p,T} = 0$. This minimization results in the equilibrium condition $h(p,T) = (\partial f/\partial\phi)_{p,T}$ and thus makes the equilibrium value of the order parameter,

$\phi = \phi_e$, to be a function of p and T. A particular form of $\phi = \phi_e(p,T)$ depends on the nature of the order parameter. Generally, one can expect that $\phi_e(p,T)$ varies between zero (alternative amorphous structure is absent) and unity (fully developed alternative amorphous structure).

2.2 Polyamorphism driven by "chemical reaction" equilibrium

To enable the general formulation of fluid polyamorphism be used for calculations of thermodynamic properties, I need to specify the nature of the order parameter and, consequently, the explicit form of the function $f(\phi)$. One attractive possibility is chemical-reaction equilibrium between two alternative thermodynamically interconvertible states, A and B. I do not specify the atomistic structure or these states. They can be two different structures of the same molecule (isomers), dissociates and associates, or two alternative supramolecular structures, such as different forms of a hydrogen-bond network. For example, cyclohexane exhibits two different configurations of molecules—either *cis* (boat) configuration or *trans* (chair) configuration. Different forms of a hydrogen-bond network are simplified to two representative forms of networks—one low density form and one high density form.

The chemical reaction is a general reaction between two structures A and B which will be controlled by a chemical reaction equilibrium constant. This chemical reaction is not necessarily a reaction in the usual sense of the word, but is a generalized chemical reaction. The chemical reaction could be a change between two structures of the same molecule, or it could be supramolecular, between two local structures, like

two different hydrogen bond networks. Configuration A has high density and high energy, and configuration B has low density and low entropy. State A is favored at higher temperatures while state B is favored at lower temperatures. The two states follow the chemical reaction

$$A \rightleftarrows B.$$

It is important to note that this chemical reaction is reversible. For the cases of this research, the reaction is assumed to always be in equilibrium. Let the fraction of state B be equal to x, also known as the reaction coordinate. This means that the reaction is assumed to be so fast that it is in equilibrium at all of the timescales I am working with. The Gibbs energy for this system follows the two state model as

$$G = (1-x)G_{\mathrm{A}} + xG_{\mathrm{B}} + G_{\mathrm{mix}} \tag{2}$$

Where where G_{A} and G_{B} are the Gibbs energies of state A and state B respectively, and G_{mix} is a general version of the Gibbs energy of mixing. By taking a simple single parameter of nonideality I obtain

$$G = G_{\mathrm{A}}(1-x) + G_{\mathrm{B}}x + kTx\ln(x) + kT(1-x)\ln(1-x) + \omega x(1-x) \tag{3}$$

where k is the Boltzmann constant, T is the temperature, x is the fraction of state B, and ω is the nonideality. If the nonideality is dependent on temperature, the mixing is purely energy driven ("regular mixing"). If the nonideality is dependent on pressure, the mixing is purely entropy driven ("athermal mixing"). For this specific case, I will take the nonideality ω to be simply a constant, determined through the critical temperature of the liquid-liquid transition ($T_{c2} = \omega/2k$). Since only state A will be formally described by an equation of state, the Gibbs energy can be simplified to

$$G = G_{\mathrm{A}} + G_{\mathrm{BA}} x + kTx\ln(x) + kT(1-x)\ln(1-x) + \omega x(1-x) \qquad (4)$$

where G_{BA} is the difference in Gibbs energies from state A and B in the form $G_{BA} = G_B - G_A$.

Now I constrain the equation using the condition for chemical reaction equilibrium between states A and B, the minimization of the Gibbs energy with respect to the reaction coordinate, *x*, of

$$\left(\frac{\partial(G/kT)}{\partial x}\right)_{p,T} = 0 \qquad (5)$$

Which will allow me to calculate the equilibrium value of $x_e = x(T, p)$ through this constraint. The full derivative of Eq. (4) through Eq. (5) simplifies to

$$\frac{G_{\mathrm{BA}}}{kT} + \ln\frac{x}{1-x} + \frac{\omega}{kT}(1-2x) = 0\,. \qquad (6)$$

This equation allows us to take the two state equation of state, which is normally for a binary fluid, and simplify it to a simple component fluid with a chemical reaction equilibrium between two states. G_{BA} can further be specified by introducing the equation

$$\ln K(T, p) = -\frac{G_{\mathrm{BA}}}{kT} \qquad (7)$$

Where *K* is the reaction equilibrium constant. Equations (6) and (7) can be simplified to

$$\ln K = \ln\frac{x}{1-x} + \frac{2T_{\mathrm{c2}}}{T}(1-2x)\,. \qquad (8)$$

In zero field, i.e. along the line $\ln K(p,T) = 0$, there is only one solution of Eq. (8), namely, if $\omega/kT \le 2$ $x = 1/2$. However, if $\omega/kT > 2$, this equation has two

stable solutions, $x > 1/2$ and $1-x < 1/2$. This corresponds to the coexistence, along the line $\ln K(T,P) = 0$, of two fluid phases, one is enriched with B and another one enriched with A. Hence the line $\ln K(T,P) = 0$ is the fluid-fluid phase transition line. The temperature

$$T_{c2} = \frac{\omega}{2k} \tag{9}$$

is the critical temperature for the polyamorphic fluid-fluid transition. The critical pressure p_{c2}, is found from the condition $\ln K\left(T = T_{c2}, p = p_{c2}\right) = 0$. The temperature of the fluid-fluid coexistence as a faction of the fraction of state B is found as

$$\hat{T}_{cxc} = \frac{2(2x-1)}{\ln x(1-x)}, \tag{10}$$

where $\hat{T}_{cxc} = T_{cxc} / T_{c2}$. At the critical point $x = x_c = 1/2$. Above the critical temperature, the line $\ln K(p,T) = 0$ (along which $x = 1/2$, a continuation of the line of phase transitions) is known as the Widom line.

Equation (10) is equivalent to temperature dependence of the spontaneous (in zero field) order parameter obtained in the mean-field approximation for the Ising/lattice gas model. Indeed, introducing $M = 2x-1$ and taking in account that $\operatorname{arctanh}(M) = \frac{1}{2}\ln\frac{1+M}{1-M}$, I obtain the famous Ising-model result:

$$M = \tanh\frac{M}{\hat{T}_{cxc}}. \tag{11}$$

Expansion of Eq. (11) in powers of *M* in the vicinity of the critical point gives in the lowest approximation $M = 2x-1 = \pm\left[\left(T - T_{c2}\right)/T_{c2}\right]^{1/2}$.

An equation of state for the system with chemical reaction equilibrium between state A and state B is written as

$$V\left(p,T\right)=\frac{1}{kT}\left(\frac{\partial G}{\partial p}\right)_{T} \tag{12}$$

Where G is the equation given in Eq. (5). By applying this equation to our Gibbs energy equation I obtain the volume per molecule as

$$V\left(p,T\right)=V_{\mathrm{A}}+xV_{\mathrm{BA}}+\frac{\partial x}{\partial p}G_{\mathrm{BA}}+kT\frac{\partial}{\partial p}\left[x\ln x+\left(1-x\right)\ln\left(1-x\right)+\frac{\omega}{kT}x\left(1-x\right)\right] \tag{13}$$

Where volume is determined through the equation of state of state A by $V_{\mathrm{A}}=V_{\mathrm{A}}\left(p,T\right)$. The additional volume term, in the form of xV_{BA}, is a function of pressure and temperature and is specified by

$$xV_{\mathrm{BA}}=x\frac{\partial G_{\mathrm{BA}}}{\partial p}=-xkT\frac{\partial\left(\ln K\right)}{\partial p} \tag{14}$$

It can be easily shown that

$$\frac{\partial x}{\partial p}G_{\mathrm{BA}}+kT\frac{\partial}{\partial p}\left[x\ln x+\left(1-x\right)\ln\left(1-x\right)+\frac{\omega}{kT}x\left(1-x\right)\right]=0\,. \tag{15}$$

The following derivation allows me to find an effective density of the system. Due to the chemical reaction constraint, the density of the overall system is shifted due to the increase of state B (lower density) at low temperatures. The effective density can be found from the above derivation through the equation

$$\rho\left(\hat{p},\hat{T}\right)=\frac{1}{V\left(\hat{p},\hat{T}\right)}=\frac{1}{V_{\mathrm{LG}}\left(\hat{p},\hat{T}\right)-5.18\left(\partial\ln K/\partial\hat{P}\right)x\left(\hat{p},\hat{T}\right)\hat{T}} \tag{16}$$

Which accounts for the density change from the normal lattice gas equation, and the chemical reaction constraint I have put on the system.

For this case, I will only specify state A with an equation of state, and state B will not be completely specified. State B will be specified through ln*K*, which is specified as a function of pressure and temperature. A generic version of ln*K* is

$$\ln K = \frac{\lambda}{T} + ap + b\frac{p}{T} + c + dT + e\frac{p^2}{T} + \ldots \qquad (17)$$

Where any number of higher order terms could be used in the specification. All of the constants shown have the following physical meanings between two states: λ is the enthalpy change, *a* is the expansivity change, *b* is the volume change, *c* is the entropy change, *d* is the heat capacity change, and *e* is the compressibility change. A specific form of ln*K* used for this thesis is

$$\ln K\left(\hat{T}, \hat{p}\right) = \left(\frac{\lambda}{\hat{T}} + \frac{b\hat{p}}{\hat{T}} + c\right) \qquad (18)$$

Which denotes a straight line on the *P*-*T* phase diagram and is a simple case to analyze.

2.3 Connection to the general formulation of fluid polyamorphism

One can notice that Eq. (4) becomes equivalent to Eq. (1) in the general formulation of fluid polyamorphism if G_A is identified with G_0, G_{BA} with $-h$, G_{mix} with $kTf(\phi)$, and the reaction coordinate *x* with the order parameter ϕ. The chemical reaction equilibrium between A and B makes the mixture of A and B thermodynamically equivalent to a single-component fluid. Indeed, the equilibrium

value of the reaction coordinate $x = x_e(T, p)$, the fraction of molecules involved in state B, is obtained from the condition of chemical reaction equilibrium

$$\left(\frac{\partial(G/kT)}{\partial x}\right)_{p,T} = 0, \qquad (19)$$

resulting in the explicit relation between the order parameter and the ordering field:

$$h = kT \ln K(p,T) = -G_{BA}(p,T) = kT \ln \frac{x}{1-x} + \omega(1-2x), \quad (20)$$

where $\ln K(T,P)$ is the reaction equilibrium constant. In a binary mixture without chemical equilibrium, because G_A and G_B are independent, the difference between the Gibbs energies, G_{BA}, depends on an arbitrary constant. The chemical-equilibrium condition Eq. (19) eliminates this uncertainty, thus making G_{BA} well defined.

An important practical question arises: under which conditions will the system described by Eq. (4) behave as a binary fluid mixture or a single-component fluid? The answer depends on the separation of time scales: a system with two inter-convertible fluid structures can be thermodynamically treated as a single-component fluid if the time of observation is longer than the characteristic time of "reaction" (fast conversion). In the opposite limit (slow conversion) the system thermodynamically behaves as a two-component mixture. In this case, constraining imposed by Eq. (19) does not apply and the concentration of species becomes an independent variable. Therefore, in order to apply the "chemical-reaction" approach for the description of fluid polyamorphism I must assume a conversion fast enough to satisfy the equilibrium condition Eq. (19) within the observation time scale.

2.4 Specifying state A: the lattice gas equation of state

For this thesis, state A will be described by the lattice gas equation of state in the mean field approximation. The lattice gas model, introduced by Frenkel in 1932 [133], is a lattice where cells can either be filled or empty. This model is particularly important in the field of physics of condensed matter because the lattice model applies to a variety of different systems and phenomena. This model can effectively bridge a gap between the physics of solid states and fluids. A schematic of this model can be seen in figure 12.

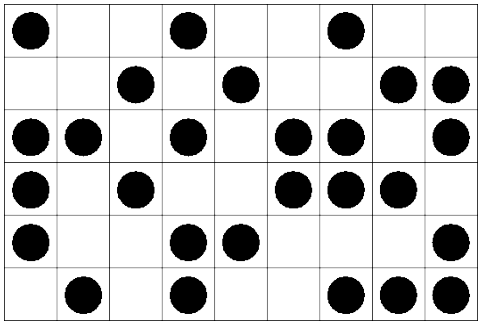

Figure 12. Two-Dimensional representation of the lattice gas.

In the lattice gas equation of state, the density can only be between 0 and 1, due to the density being made dimensionless with respect to the number of cells occupied. This density then is a fraction between 0 and 1 of cells occupied. Further, while exact analytical solutions of the three-dimensional lattice gas models are not available, numerical approximations give good accuracy. The mean field approximation is one of these numerical solutions to the three-dimensional lattice gas model. The mean field approximation denotes all of the multi-body interactions in the system to a single

parameter, ε. This approximation is similar to the van der Waals fluid by the interaction constant *a*, while the role of the van der Waals constant *b*, the molecular volume constant, in the lattice gas is played by the dimensionless density. The lattice gas equation of state in the mean field approximation is

$$p = -kT\ln\left(1-\rho\right)-\varepsilon\rho^2 \tag{21}$$

where p is the pressure (in units of energy), ε is a constant determined by the critical temperature of the vapor-liquid transition ($T_{C1} = \varepsilon/2k$), k is the Boltzmann constant, T is the temperature, and ρ is the density (dimensionless). The chemical potential of the lattice gas is

$$\mu = kT\ln\frac{\rho}{1-\rho}-2\varepsilon\rho+\varepsilon \tag{22}$$

Where μ is the chemical potential, and all other variables are the same as for the pressure equation. Additionally the density of the Helmholtz energy ($\rho a \equiv \rho A/N = \rho\mu - P$) will be useful when looking to analyze the phase behavior of the lattice gas model. The density of the Helmholtz energy is written as

$$\rho a = \rho\mu - p = kT\rho\ln\rho + kT\left(1-\rho\right)\ln\left(1-\rho\right)+\varepsilon\rho\left(1-\rho\right) \tag{23}$$

Where a is the Helmholtz energy. This function can be made symmetric by subtracting the linear dependence with respect to the density. This allows for the condition of fluid phase equilibria (the binodal) to be symmetric as well, as opposed to the asymmetric nature of the van der Waals fluid. The binodal can be calculated through the condition

$$\mu_{\text{eq}} - \varepsilon = kT\ln\frac{\rho}{1-\rho}-2\varepsilon\rho = 0\,. \tag{24}$$

Therefore, the spinodal (limit of absolute mechanical stability) can be calculated through the condition

$$\left(\frac{\partial \mu}{\partial \rho}\right)_T = \frac{kT}{\rho(1-\rho)} - 2\varepsilon = 0 . \qquad (25)$$

The critical point parameters in the lattice gas model are $\rho_{c1} = 1/2$, $T_{c1} = \varepsilon / 2k$, and $p_{c1} = kT_{c1}\left[-\ln(1/2) - 1/2\right] \cong 0.193 kT_{c1}$. The lattice gas equation of state was made dimensionless with respect to the vapor-liquid critical point and takes the form

$$\hat{p} = \frac{\hat{T}\ln(1-\rho) + 2\rho^2}{\ln\frac{1}{2} + \frac{1}{2}} \cong -5.18\left[\hat{T}\ln(1-\rho) + 2\rho^2\right] \qquad (26)$$

Where pressure and temperature are reduced with the equations $\hat{T} = T / T_{c1}$, $\hat{p} = p_{c1}$ and T_{c1} is the critical temperature of the vapor-liquid transition, and p_{c1} is the critical pressure of the vapor-liquid transition. With these conditions, the vapor-liquid spinodal is

$$\hat{T}_{sp} = 4\rho(1-\rho) \qquad (27)$$

And the vapor-liquid coexistence is

$$\frac{1}{\hat{T}_{cxc}} = \frac{\frac{1}{2}\ln\frac{\rho}{1-\rho}}{2\rho - 1} . \qquad (28)$$

Phase behavior in the temperature-density diagram and the pressure-density diagram are shown in figures 13 and 14 below. These figures also show the properties of the lattice gas model as discussed in this section.

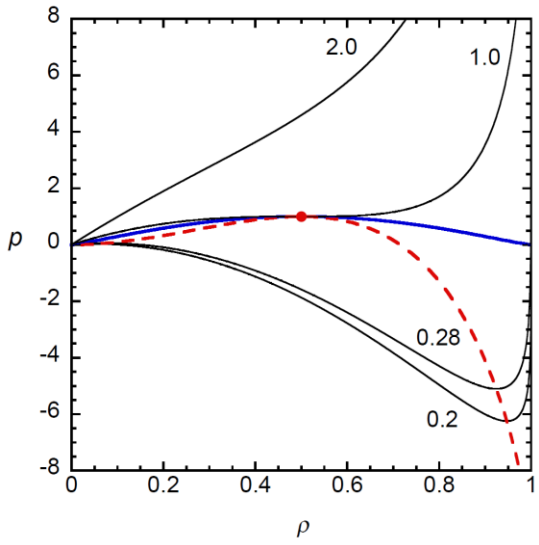

Figure 13**.** Selected isotherms and liquid-vapor coexistence of the lattice-gas model. Sold blue is binodal. Dashed red is spinodal. Red dot is the liquid-vapor critical point.

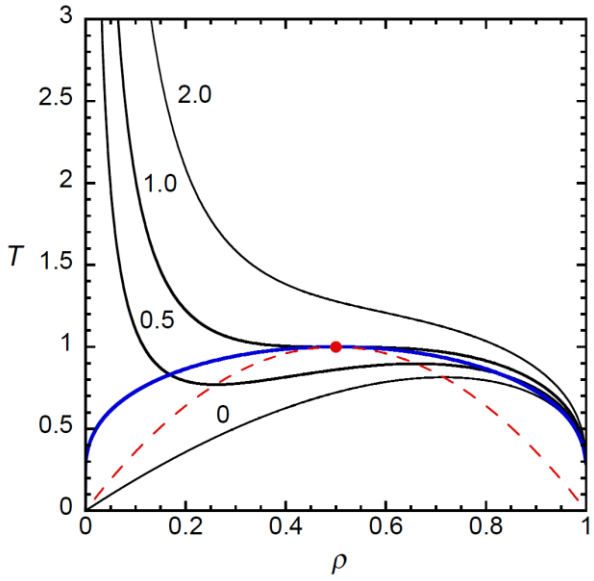

Figure 14**.** Selected isobars and liquid-vapor coexistence of the lattice-gas model. Solid blue is binodal. Dashed red is spinodal. Red dot is the liquid-vapor critical point.

Chapter 3: Global phase diagram of a polyamorphic fluid and thermodynamic properties

3.1 Calculation of the phase diagram and isothermal compressibility

For the state A I adopt the lattice-gas model, thus the Gibbs energy of the state A $G_{\mathrm{A}} \equiv \mu$, the function given by Eq. (24). Also, I use the temperature/pressure scale reduced to the critical parameters of state A, so that $\hat{T}^{*} = T_{\mathrm{c2}} / T_{\mathrm{c1}}$ and $\hat{p}^{*} = p_{\mathrm{c2}} / p_{\mathrm{c1}}$. The

$$\ln K = \ln \frac{x}{1-x} + \frac{2nT_{\mathrm{C2}}}{T}\left(1-2x\right), \qquad (29)$$

where $n = T_{C2} / T_{C1}$. Since I consider the possibility of a liquid-liquid transition, I assume

$n < 1$.

The effective density is calculated as

$$\rho\left(\hat{p},\hat{T}\right) = \frac{1}{V\left(\hat{p},\hat{T}\right)} = \frac{1}{V_{\mathrm{LG}}\left(\hat{p},\hat{T}\right) - 5.18\left(\partial \ln K / \partial \hat{P}\right) x\left(\hat{p},\hat{T}\right)\hat{T}} . \qquad (30)$$

Finally, the equation of state for the lattice gas with "chemical reaction" takes the same form as Eq. (4), but with the density calculated from Eq. (30). This density is a function of *p* and *T*, constrained by the equilibrium between the alternative states A and B. Note that $V_{\mathrm{BA}} << V_{\mathrm{LG}}$ at large volumes and very low temperatures, thus the saturation pressure curve as a function of temperature, as well as the gas branch of the gas-liquid spinodal, is not affected by the liquid-liquid transition.

The next step is to adopt a particular shape for the function $\ln K\left(T, p\right)$. A simple function which accounts for a temperature-independent heat of reaction,

$$\Delta H = kT^2 \left(\frac{\partial G_{\mathrm{BA}} / kT}{\partial T} \right)_p = kT^2 \left(\frac{\partial \ln K}{\partial T} \right)_p , \tag{31}$$

and a pressure-independent volume change of reaction,

$$V_{\mathrm{BA}} = \left(\frac{\partial G_{\mathrm{BA}}}{\partial p} \right)_T = kT \left(\frac{\partial \ln K}{\partial p} \right)_T , \tag{32}$$

is the following:

$$\ln K\left(\hat{T}, \hat{p}\right) = \lambda \left(\frac{1}{\hat{T}} + a\hat{p} + \frac{b\hat{p}}{\hat{T}} + c \right), \tag{33}$$

where $\lambda = -\Delta H / kT > 0$. A specific form of ln*K* used for this thesis is

$$\ln K\left(\hat{T}, \hat{p}\right) = \left(\frac{\lambda}{\hat{T}} + \frac{b\hat{p}}{\hat{T}} + c \right) \tag{34}$$

Which denotes a straight line on the *P*-*T* phase diagram and is a simple case to analyze. The equations derived previously are solved numerically with a Python code developed by M. Duška (Appendix A). Numerical solutions were obtained through the bisection method and Brent's method. Brent's method utilized either an inverse quadratic extrapolation term or a hyperbolic extrapolation term.

The phase diagram of a polyamorphic fluid for this specific form of ln*K* is shown in figures 15 and 16. The Widom line is an extension of the ln*K*=0 line into the single phase region and is the line where the fraction of both species A and B is equal to 50%.

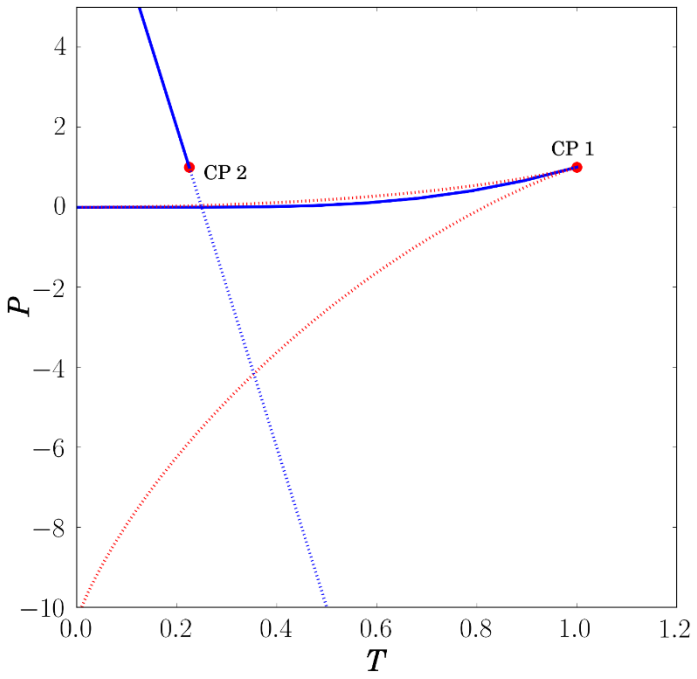

Figure 15. Phase diagram of a polyamorphic fluid. Blue curves are the vapor-liquid and liquid-liquid coexistences, terminating at the critical points (red dots) CP 1 and CP 2, respectively. Red dashed lines are the vapor-liquid spinodal branches. Blue dashed line is the Widom line of the liquid-liquid coexistence.

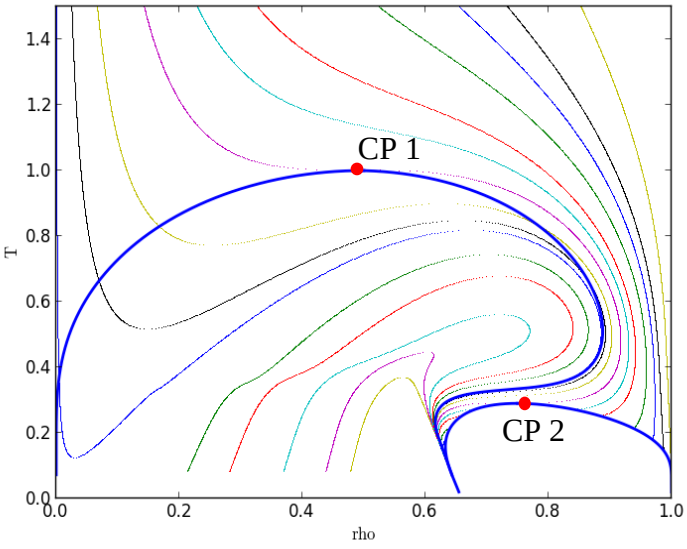

Figure 16. Temperature density diagram of a polyamorphic fluid. CP 1 and CP 2 designate the critical point of the vapor-liquid and liquid-liquid transitions, respectively. Multicolor curves show isobars including those located in the unstable region.

An important anomaly of all polyamorphic fluids is the increase of the isothermal compressibility in the proximity of the liquid-liquid transition. Figure 17a shows isobars of the compressibility as a function of temperature, with each temperature color coded. Figure 17b also shows the phase diagram of this system with each temperature shown, also color coded. The compressibility clearly behaves as expected, diverging at each critical point at the critical pressure isobar, exhibiting a maximum at the liquid-liquid transition line and then a gradual increase above the critical pressure, and exhibiting a local maximum at the Widom line and diverging at the vapor-liquid spinodal for below the critical pressure.

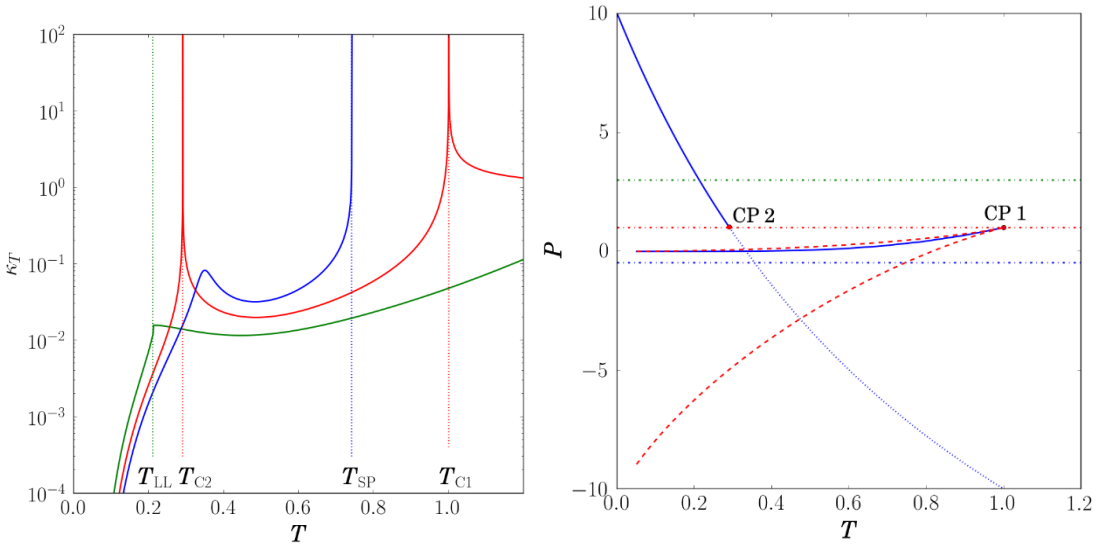

Figure 17. Compressibility of three isobars (less than critical, critical, greater than critical) are the blue, red and green curves respectively. Vapor-liquid and liquid-liquid critical points are labeled and Temperatures at the coexistence of vapor-liquid and liquid-liquid are labeled.

3.2 Tuning the nonideality of two states

In this section, I demonstrate how the tuning of the nonideality parameter ω changes the location of the liquid-liquid critical point from 0 K (ideal mixing) to the intersection with the absolute stability limit of the stretched liquid with respect to vapor. It is shown that the intersection of the liquid-liquid phase transition line with the absolute stability limit produces a specific form of the phase diagram not considered before.

The simple linear case for ln$K$ was analyzed by changing two important parameters—the reaction energy change between two states (λ), and the critical temperature of the liquid-liquid transition ($T_{c2} = \omega/2k$). The other parameters, b and c, were kept constant at the adopted values 0.05 and -2.0, respectively. Eighteen total cases were considered as summarized in Table A.1. Cases are divided into three groups (A, B, and C) corresponding to three different energy changes between two states ($\lambda = 0.1$, $\lambda = 0.5$, and $\lambda = 1$) and six values for $T_{c2} = \omega/2k$.

In particular, it is interesting to follow the evolution of extrema of thermodynamic properties. The three lines of extrema that are of interest for this thesis are density, compressibility and heat capacity. The temperatures of maximum/minimum density can be calculated through

$$\left(\frac{\partial \rho}{\partial T}\right)_p = 0 \qquad (35)$$

Where the maximum value is solved numerically for a variety of isobars. The isothermal compressibility lines of maxima and minima along isobars are calculated by calculating the values of compressibility through

$$\left(\frac{\partial \kappa_T}{\partial T}\right)_p = 0 \qquad (36)$$

Where $\kappa_T = -(1/V)(\partial V/\partial p)_T$ is the isothermal compressibility, and V is the volume per molecule, taken to be the inverse of the density ($V = 1/\rho$). Finally, the heat capacity maxima and minima along isotherms must be calculated through the thermodynamic Maxwell relation

$$\left(\frac{\partial C_p}{\partial p}\right)_T = -\left(\frac{\partial^2 V}{\partial T^2}\right)_p = 0\,. \qquad (37)$$

The cases analyze the effect that the distance between the liquid-liquid critical point and the vapor-liquid spinodal has on the pattern of the extrema lines. The first three cases of importance are cases A1, B1, and C1. These specific cases correspond to the ideal solution mixing of two states. A liquid-liquid phase transition does not exist. Figures 18, 19, and 20 depict the three ideal solution cases for three different values of λ. The main effect of the increase of energy change of reaction is shifting the pattern of the extrema lines and the Widom line to higher pressures and higher temperatures.

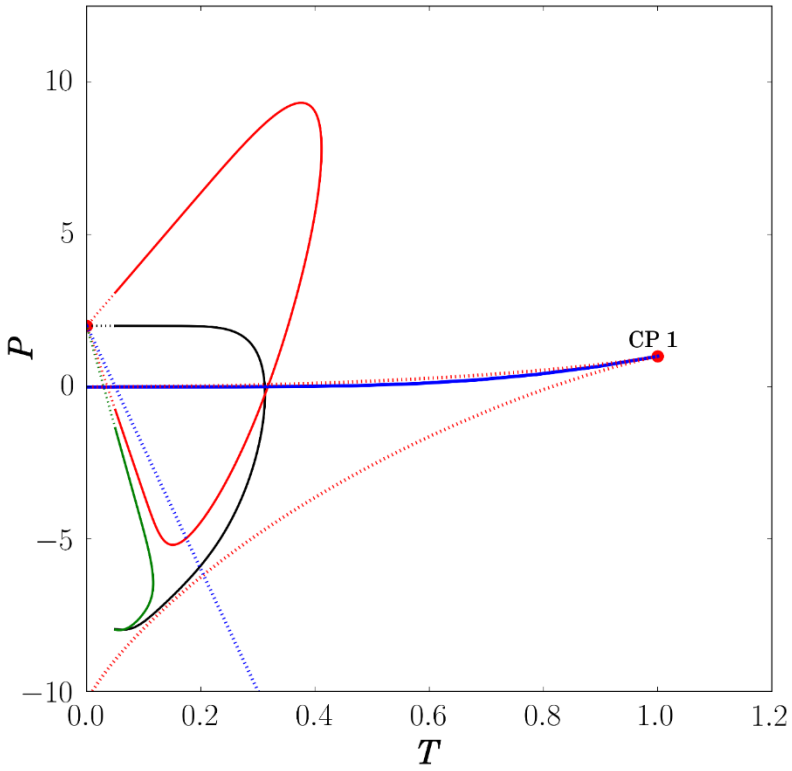

Figure 18. Case A1 phase diagram and lines of extrema. Blue curves are the vapor-liquid and liquid-liquid coexistences, terminating at the red dots CP 1 and CP 2 respectively. Red dashed lines are the vapor-liquid spinodal. Blue dashed line is the Widom line of the liquid-liquid coexistence. Red solid curve is the line of maximum and minimum compressibility. Black solid curve is the maximum and minimum density line. Green solid curve is the maximum and minimum heat capacity.

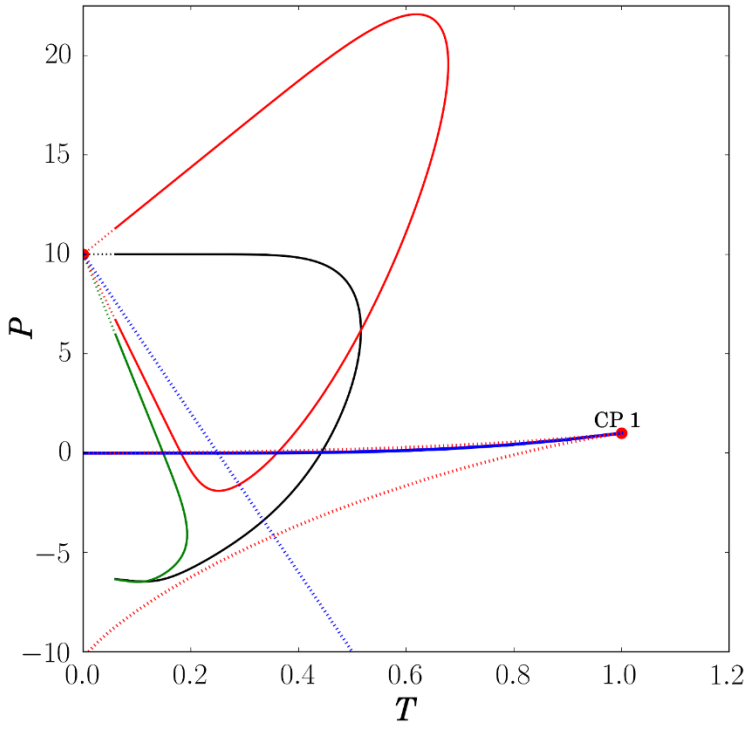

Figure 19. Case B1 phase diagram and lines of extrema. Blue curves are the vapor-liquid and liquid-liquid coexistences, terminating at the red dots CP 1 and CP 2 respectively. Red dashed lines are the vapor-liquid spinodal. Blue dashed line is the Widom line of the liquid-liquid coexistence. Red solid curve is the line of maximum and minimum compressibility. Black solid curve is the maximum and minimum density line. Green solid curve is the maximum and minimum heat capacity.

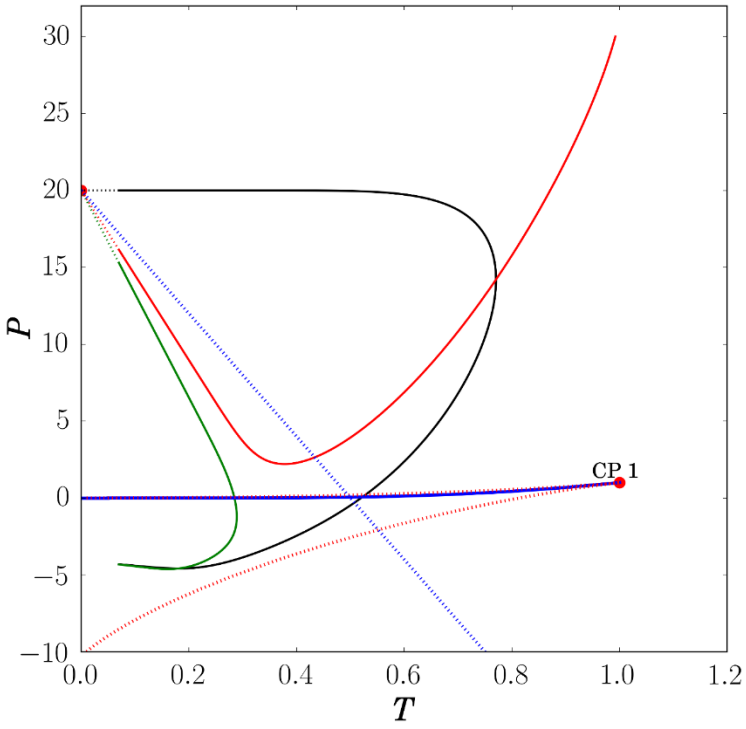

Figure 20. Case C1 phase diagram and lines of extrema. Blue curves are the vapor-liquid and liquid-liquid coexistences, terminating at the red dots CP 1 and CP 2 respectively. Red dashed lines are the vapor-liquid spinodal. Blue dashed line is the Widom line of the liquid-liquid coexistence. Red solid curve is the line of maximum and minimum compressibility. Black solid curve is the maximum and minimum density line. Green solid curve is the maximum and minimum heat capacity.

The second set of parameters, cases A2, B2, and C2, corresponds to the position of the critical point expected in some models of supercooled water. A higher energy change of reaction corresponds to a higher temperature of the second critical point and the Widom line. These cases are the first of the cases where the analysis of this equation of state is important. The critical point in each of these cases is closer to the vapor-liquid spinodal, and the patterns of extrema lines are slightly condensed. Figures 21, 22, and 23 show the three cases with the liquid-liquid critical point at P_{c2}=1.

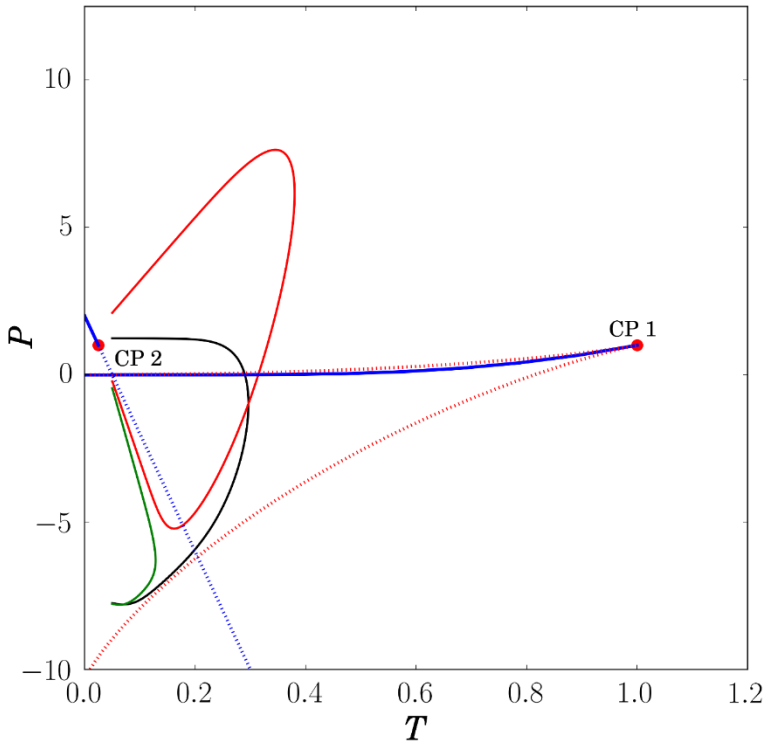

Figure 21. Case A2 phase diagram and lines of extrema. Blue curves are the vapor-liquid and liquid-liquid coexistences, terminating at the red dots CP 1 and CP 2 respectively. Red dashed lines are the vapor-liquid spinodal. Blue dashed line is the Widom line of the liquid-liquid coexistence. Red solid curve is the line of maximum and minimum compressibility. Black solid curve is the maximum and minimum density line. Green solid curve is the maximum and minimum heat capacity.

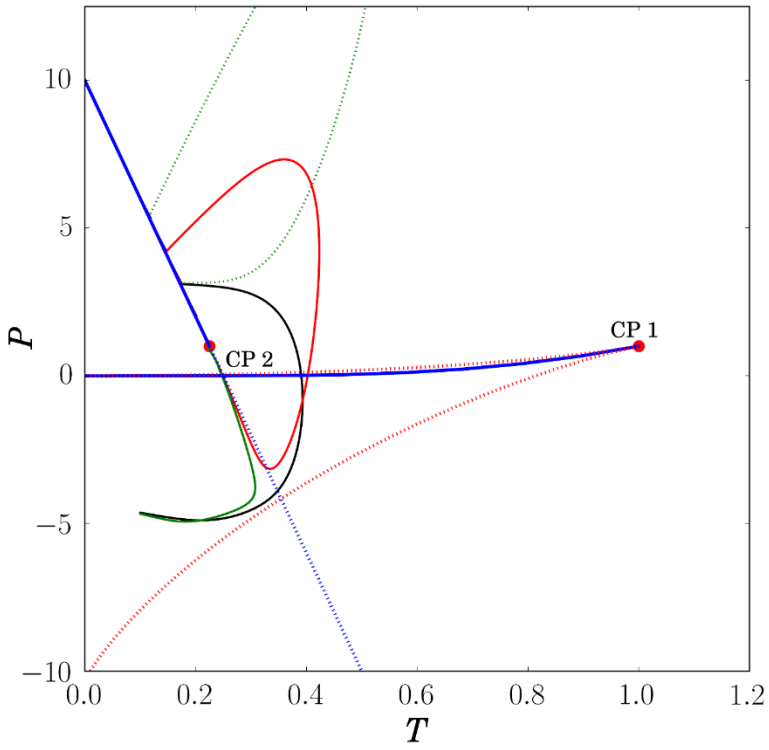

Figure 22. Case B2 phase diagram and lines of extrema. Blue curves are the vapor-liquid and liquid-liquid coexistences, terminating at the red dots CP 1 and CP 2 respectively. Red dashed lines are the vapor-liquid spinodal. Blue dashed line is the Widom line of the liquid-liquid coexistence. Red solid curve is the line of maximum and minimum compressibility. Black solid curve is the maximum and minimum density line. Green solid curve is the maximum and minimum heat capacity.

One may notice that the pattern of the extrema lines are remarkably similar to those obtained from MD simulations from ST2 and TIP4P/2005 presented in figure 6. Furthermore, like in the results of the simulation studies, the vapor-liquid spinodal does not significantly affect the behavior of the extrema lines.

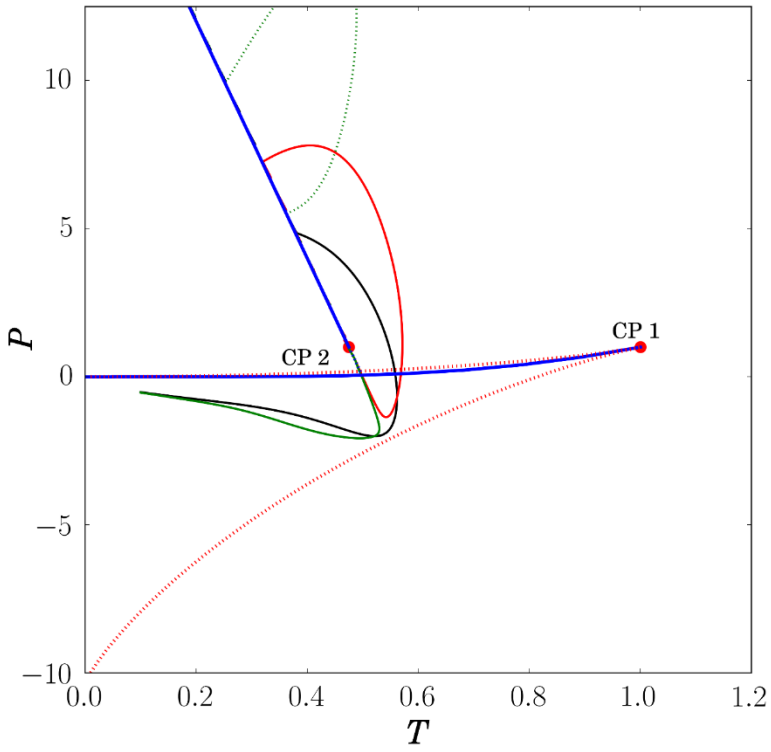

Figure 23. Case C2 phase diagram and lines of extrema. Blue curves are the vapor-liquid and liquid-liquid coexistences, terminating at the red dots CP 1 and CP 2 respectively. Red dashed lines are the vapor-liquid spinodal. Blue dashed line is the Widom line of the liquid-liquid coexistence. Red solid curve is the line of maximum and minimum compressibility. Black solid curve is the maximum and minimum density line. Green solid curve is the maximum and minimum heat capacity.

The third set of cases are cases A3, B3, and C3. These cases are where the liquid-liquid critical point is located at exactly where the vapor-liquid coexistence is for the first critical point. Again, each critical point is closer to the vapor-liquid spinodal, but still the patterns of the extrema lines are similar to cases A2, B2, and C2. Figures 24, 25, and 26 show the cases described.

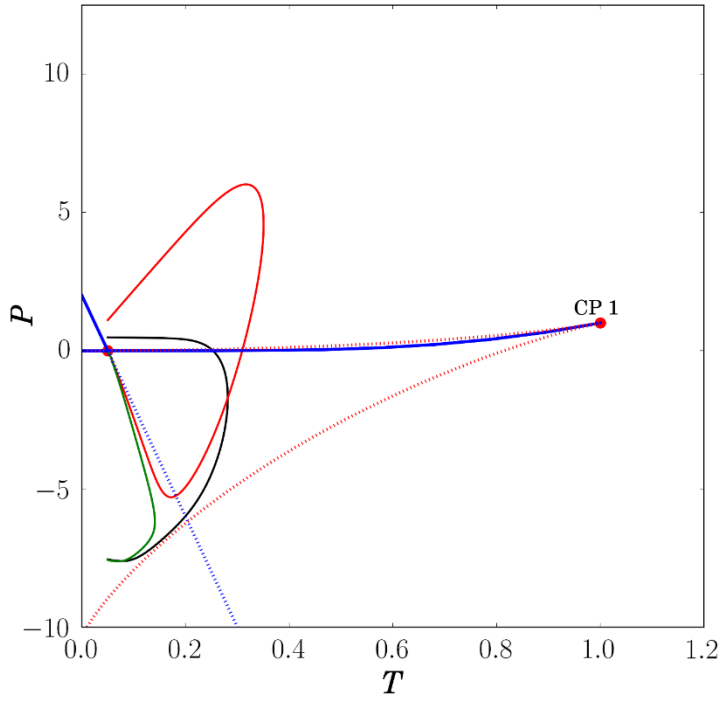

Figure 24. Case A3 phase diagram and lines of extrema. Blue curves are the vapor-liquid and liquid-liquid coexistences, terminating at the red dots CP 1 and CP 2 respectively. Red dashed lines are the vapor-liquid spinodal. Blue dashed line is the Widom line of the liquid-liquid coexistence. Red solid curve is the line of maximum and minimum compressibility. Black solid curve is the maximum and minimum density line. Green solid curve is the maximum and minimum heat capacity.

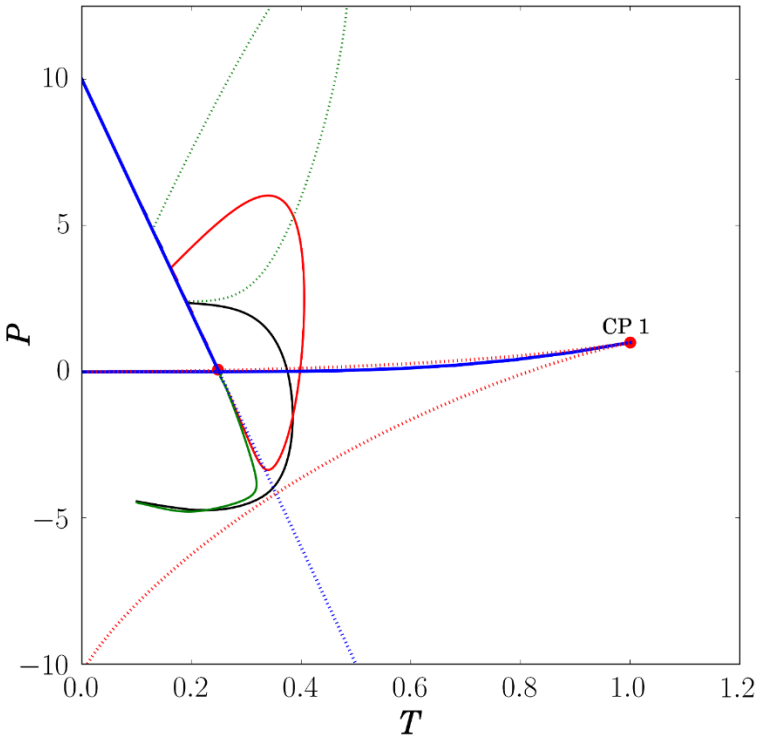

Figure 25. Case B3 phase diagram and lines of extrema. Blue curves are the vapor-liquid and liquid-liquid coexistences, terminating at the red dots CP 1 and CP 2 respectively. Red dashed lines are the vapor-liquid spinodal. Blue dashed line is the Widom line of the liquid-liquid coexistence. Red solid curve is the line of maximum and minimum compressibility. Black solid curve is the maximum and minimum density line. Green solid curve is the maximum and minimum heat capacity.

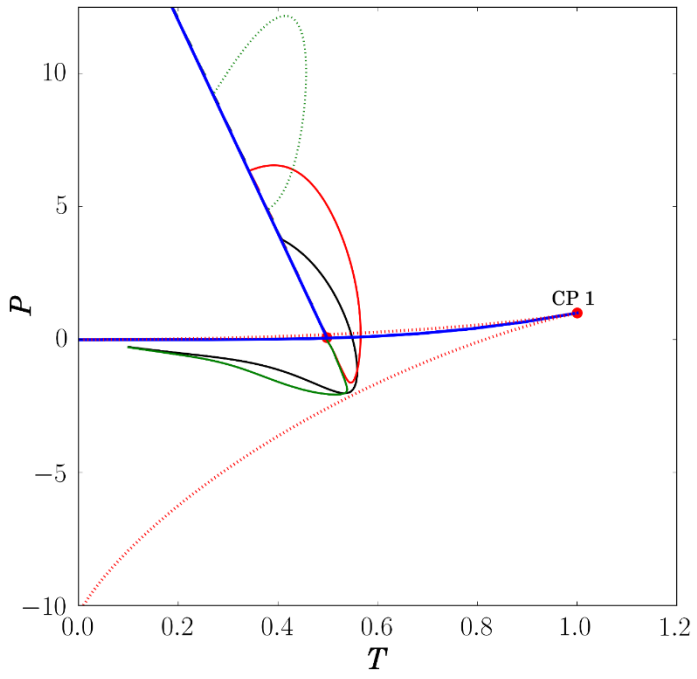

Figure 26. Case C3 phase diagram and lines of extrema. Blue curves are the vapor-liquid and liquid-liquid coexistences, terminating at the red dots CP 1 and CP 2 respectively. Red dashed lines are the vapor-liquid spinodal. Blue dashed line is the Widom line of the liquid-liquid coexistence. Red solid curve is the line of maximum and minimum compressibility. Black solid curve is the maximum and minimum density line. Green solid curve is the maximum and minimum heat capacity.

Cases A4, B4, and C4 show the cases where the critical point of the liquid-liquid transition is located at a pressure below zero. In these cases, the critical point is located in the doubly metastable region—where the water is metastable with respect to both vapor and solid. A particular feature to notice in these plots is the beginning of the collapse of the extrema lines onto the liquid-liquid transition line. Particularly, the line of maximum density is quickly collapsing onto the liquid-liquid transition line. Figures 27, 28, and 29 show these cases below.

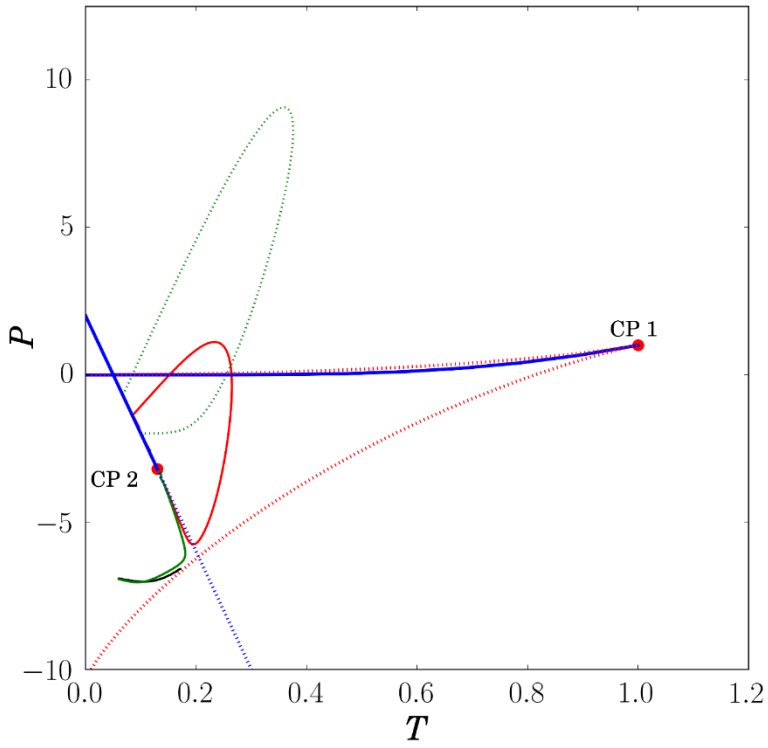

Figure 27. Case A4 phase diagram and lines of extrema. Blue curves are the vapor-liquid and liquid-liquid coexistences, terminating at the red dots CP 1 and CP 2 respectively. Red dashed lines are the vapor-liquid spinodal. Blue dashed line is the Widom line of the liquid-liquid coexistence. Red solid curve is the line of maximum and minimum compressibility. Black solid curve is the maximum and minimum density line. Green solid curve is the maximum and minimum heat capacity.

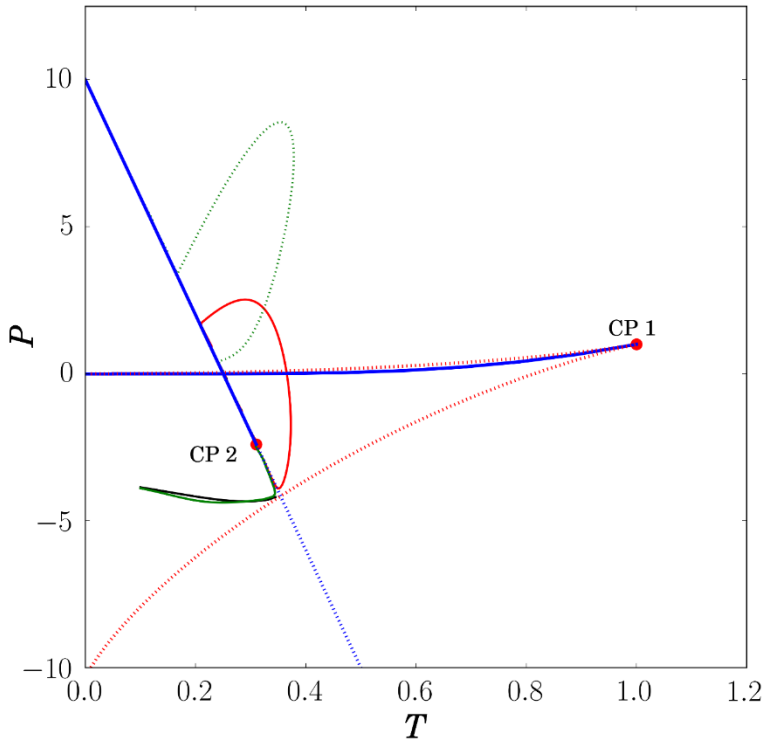

Figure 28. Case B4 phase diagram and lines of extrema. Blue curves are the vapor-liquid and liquid-liquid coexistences, terminating at the red dots CP 1 and CP 2 respectively. Red dashed lines are the vapor-liquid spinodal. Blue dashed line is the Widom line of the liquid-liquid coexistence. Red solid curve is the line of maximum and minimum compressibility. Black solid curve is the maximum and minimum density line. Green solid curve is the maximum and minimum heat capacity.

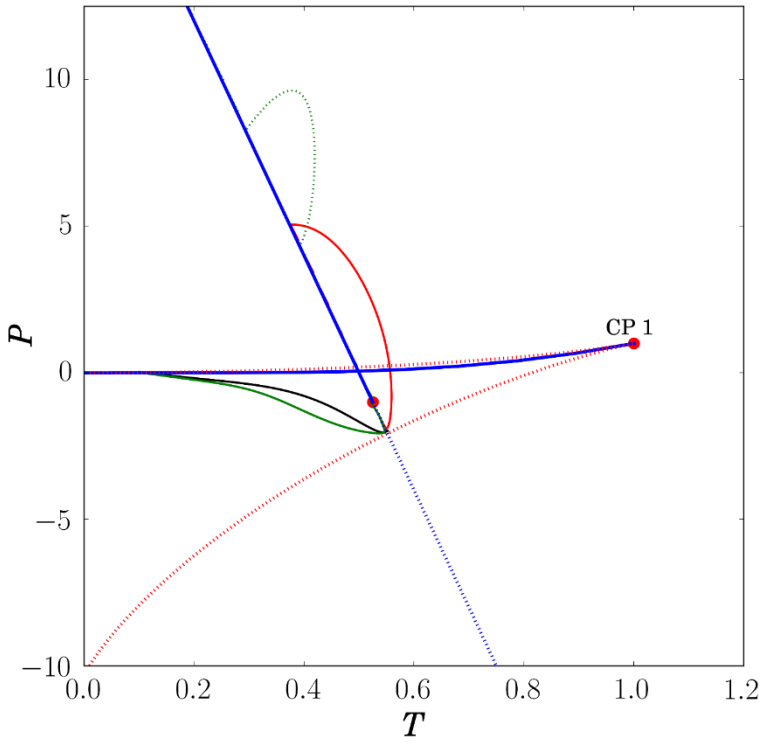

Figure 29. Case C4 phase diagram and lines of extrema. Blue curves are the vapor-liquid and liquid-liquid coexistences, terminating at the red dots CP 1 and CP 2 respectively. Red dashed lines are the vapor-liquid spinodal. Blue dashed line is the Widom line of the liquid-liquid coexistence. Red solid curve is the line of maximum and minimum compressibility. Black solid curve is the maximum and minimum density line. Green solid curve is the maximum and minimum heat capacity.

The next cases considered were cases A5, B5, and C5. These cases show where the liquid-liquid critical point intersects the vapor-liquid spinodal. This is the most interesting case because the liquid-liquid transition is terminated at exactly the limit of stability for the entire liquid phase. Again, the lines of extrema are collapsing onto the liquid-liquid transition line and without zooming in, it appears that the density maxima has completely disappeared. Figures 30, 31 and 32 depict these cases below.

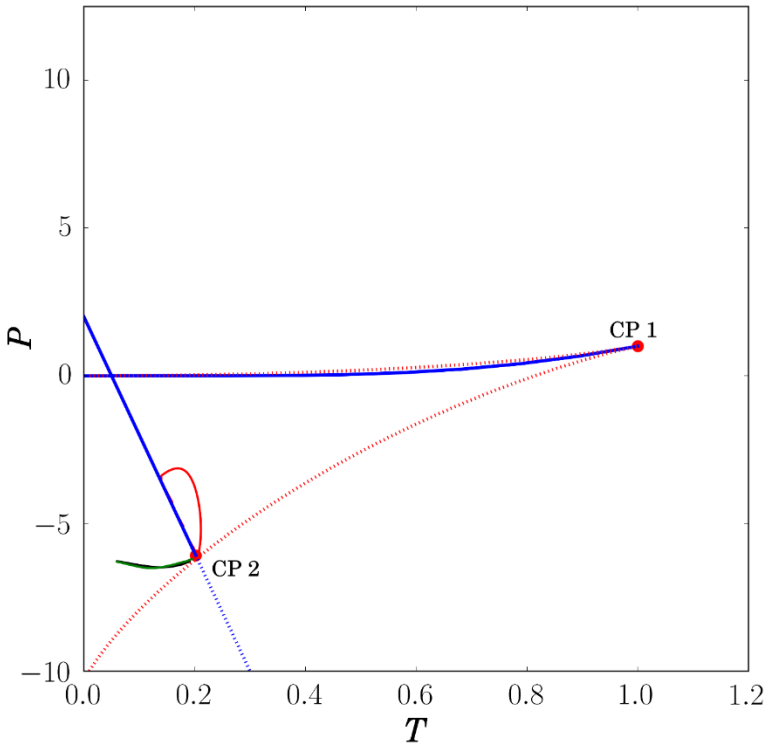

Figure 30. Case A5 phase diagram and lines of extrema. Blue curves are the vapor-liquid and liquid-liquid coexistences, terminating at the red dots CP 1 and CP 2 respectively. Red dashed lines are the vapor-liquid spinodal. Blue dashed line is the Widom line of the liquid-liquid coexistence. Red solid curve is the line of maximum and minimum compressibility. Black solid curve is the maximum and minimum density line. Green solid curve is the maximum and minimum heat capacity.

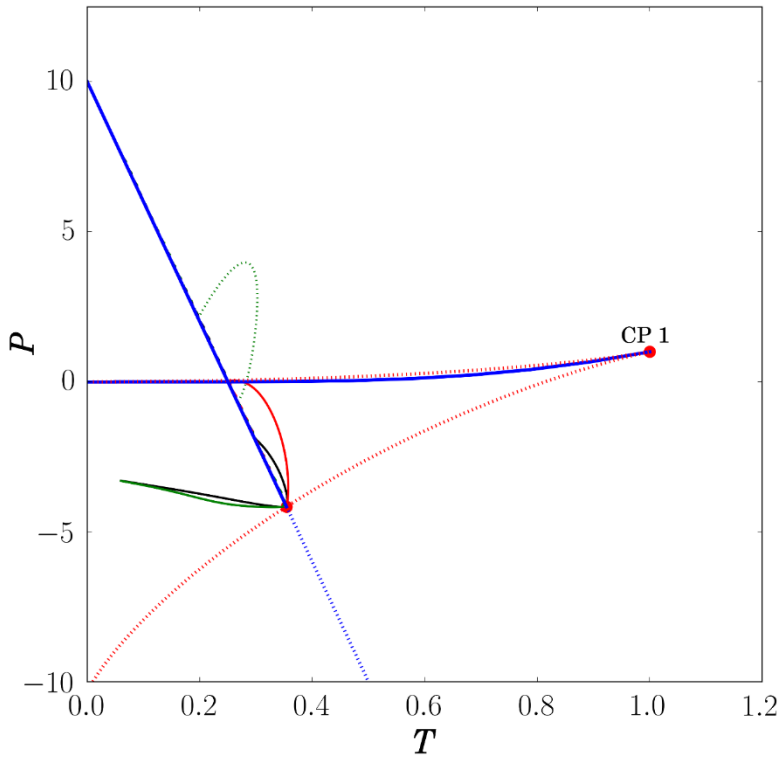

Figure 31. Case B5 phase diagram and lines of extrema. Blue curves are the vapor-liquid and liquid-liquid coexistences, terminating at the red dots CP 1 and CP 2 respectively. Red dashed lines are the vapor-liquid spinodal. Blue dashed line is the Widom line of the liquid-liquid coexistence. Red solid curve is the line of maximum and minimum compressibility. Black solid curve is the maximum and minimum density line. Green solid curve is the maximum and minimum heat capacity.

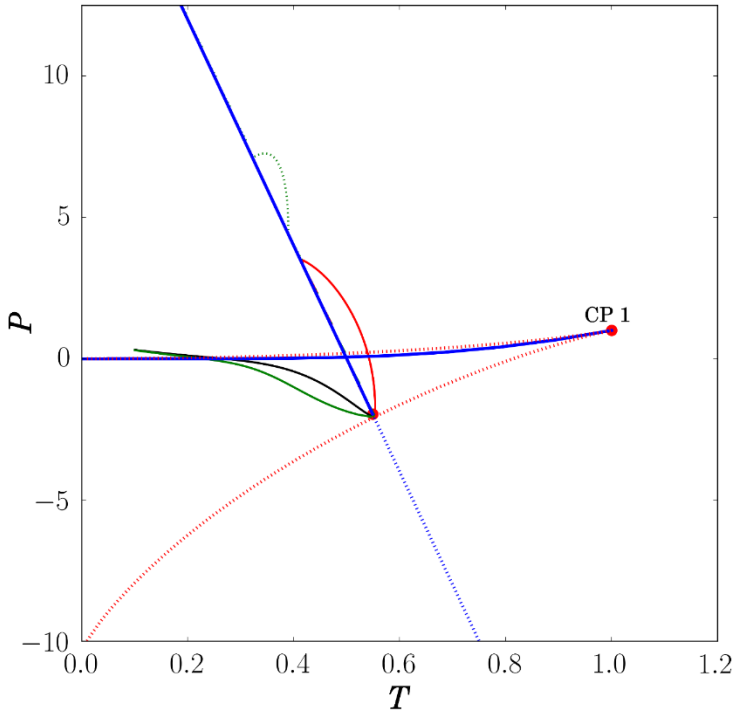

Figure 32. Case C5 phase diagram and lines of extrema. Blue curves are the vapor-liquid and liquid-liquid coexistences, terminating at the red dots CP 1 and CP 2 respectively. Red dashed lines are the vapor-liquid spinodal. Blue dashed line is the Widom line of the liquid-liquid coexistence. Red solid curve is the line of maximum and minimum compressibility. Black solid curve is the maximum and minimum density line. Green solid curve is the maximum and minimum heat capacity.

The final cases considered were cases A6, B6, and C6. These cases are for a liquid-liquid critical point below the limit of absolute stability, or in other words correspond to a transition where there is a line of critical points at the transition line for all temperatures. The figures here show a collapse of nearly all extrema lines onto the liquid-liquid transition line. These lines do not match what the simulations have predicted for water models (figure 6). This result can confirm that the critical-point-free scenario of a liquid-liquid transition line that has no terminating critical point can be excluded because in this case, the density extrema line almost disappears, while

being very pronounced for supercooled water. Figures 33, 34, and 35 show these final cases.

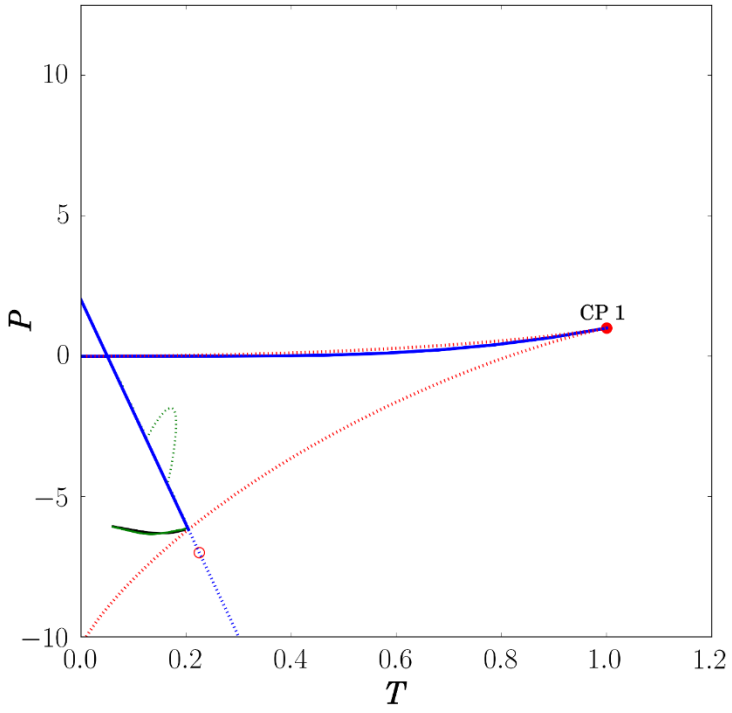

Figure 33. Case A6 phase diagram and lines of extrema. Blue curves are the vapor-liquid and liquid-liquid coexistences, terminating at the red dots CP 1 and CP 2 respectively. Red dashed lines are the vapor-liquid spinodal. Blue dashed line is the Widom line of the liquid-liquid coexistence. Red solid curve is the line of maximum and minimum compressibility. Black solid curve is the maximum and minimum density line. Green solid curve is the maximum and minimum heat capacity.

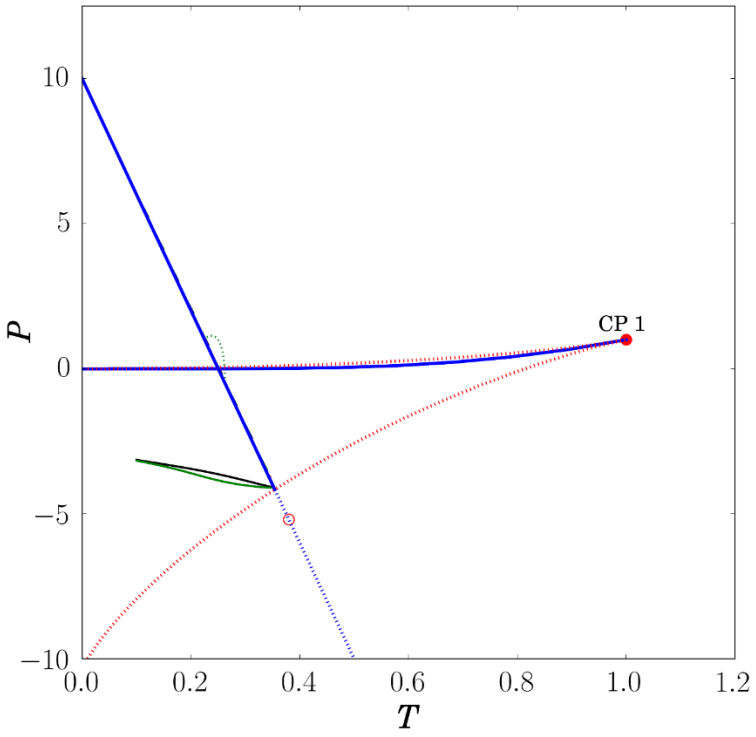

Figure 34. Case B6 phase diagram and lines of extrema. Blue curves are the vapor-liquid and liquid-liquid coexistences, terminating at the red dots CP 1 and CP 2 respectively. Red dashed lines are the vapor-liquid spinodal. Blue dashed line is the Widom line of the liquid-liquid coexistence. Red solid curve is the line of maximum and minimum compressibility. Black solid curve is the maximum and minimum density line. Green solid curve is the maximum and minimum heat capacity.

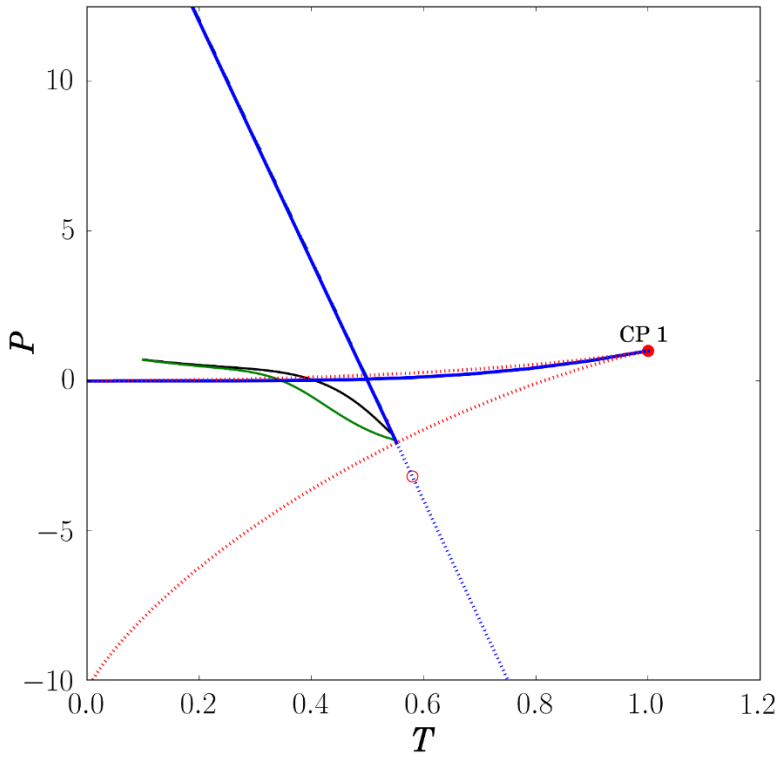

Figure 35. Case C6 phase diagram and lines of extrema. Blue curves are the vapor-liquid and liquid-liquid coexistences, terminating at the red dots CP 1 and CP 2 respectively. Red dashed lines are the vapor-liquid spinodal. Blue dashed line is the Widom line of the liquid-liquid coexistence. Red solid curve is the line of maximum and minimum compressibility. Black solid curve is the maximum and minimum density line. Green solid curve is the maximum and minimum heat capacity.

The further analysis of the case where the liquid-liquid critical point touches the absolute stability limit of liquid state has found a novel thermodynamic feature that becomes present in temperature-density and pressure-density diagrams. The liquid-liquid coexistence exhibits a bird's beak at the critical point. This is because the critical point touches the spinodal exactly and forces the slope of the liquid-liquid coexistence to be exactly the same as the spinodal at the critical point. Figures 36 and 37 illustrate this interesting phenomenon.

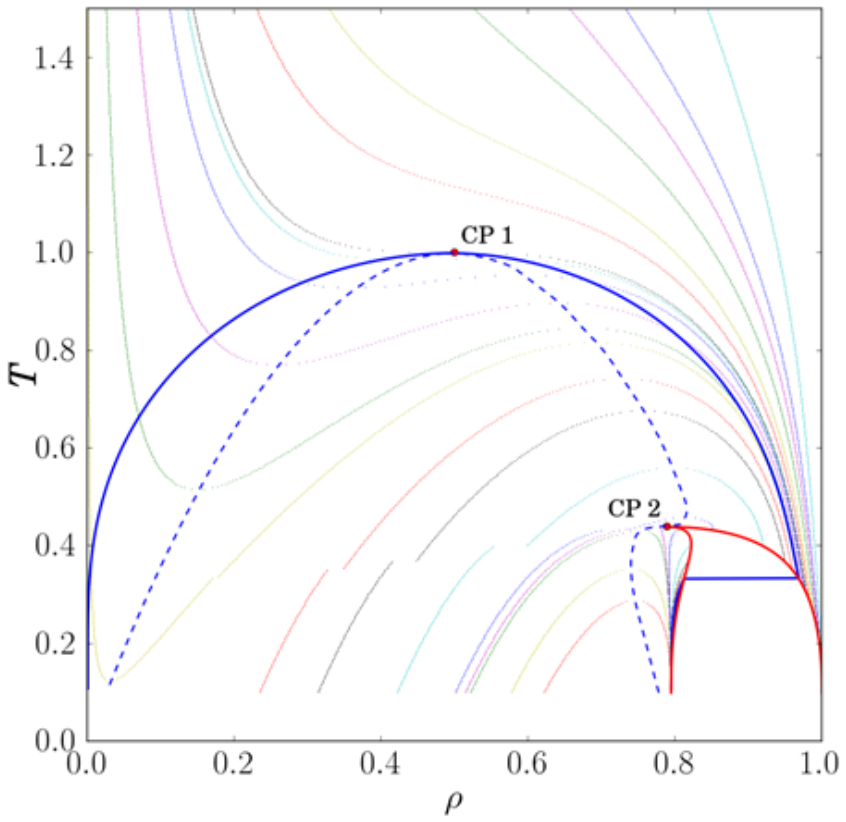

Figure 36. Phase diagram showing temperatures of isobars with respect to density. Specifically for the case where the CP 2 is directly touching the vapor-liquid spinodal. Multicolored lines are isobars. Blue solid curve is the vapor-liquid coexistence. Blue dotted curve is the vapor-liquid spinodal. Red solid curve is the liquid-liquid coexistence, clearly showing a bird's beak type of phenomenon. CP 1 and CP 2 are labeled in black.

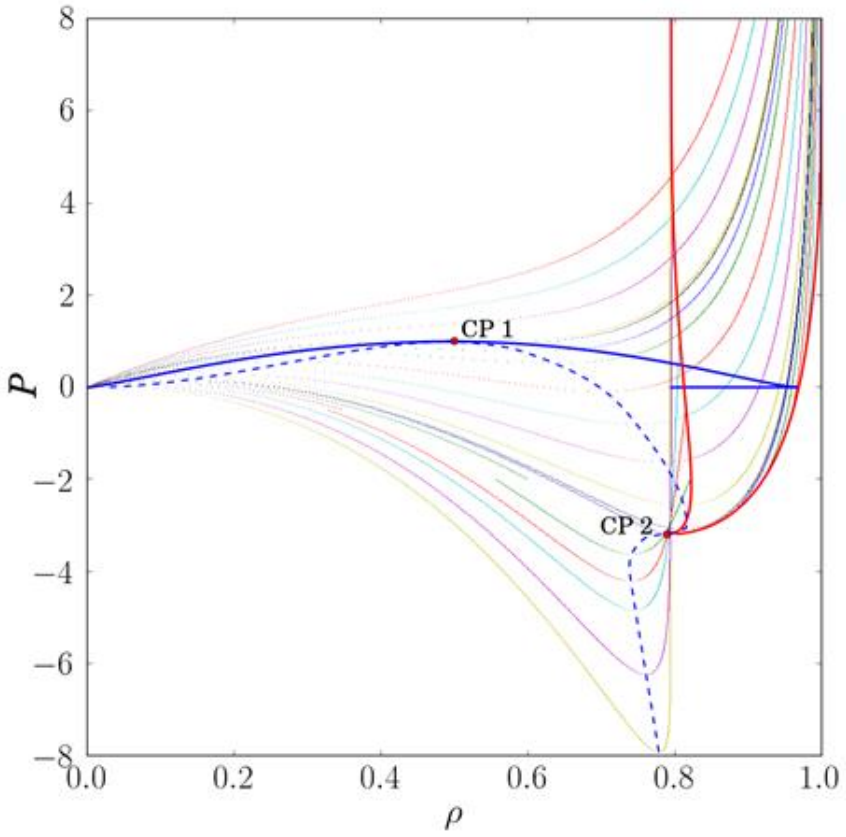

Figure 37. Phase diagram showing pressures of isotherms with respect to density. Specifically for the case where the CP 2 is directly touching the vapor-liquid spinodal. Multicolored lines are isobars. Blue solid curve is the vapor-liquid coexistence. Blue dotted curve is the vapor-liquid spinodal. Red solid curve is the liquid-liquid coexistence, clearly showing a bird's beak type of phenomenon. CP 1 and CP 2 are labeled in black.

Chapter 4: Discussion

The "chemical reaction" approach to fluid polyamorphism discussed in this thesis uses equilibrium thermodynamics to phenomenologically describe a phase transition. This approach can be analogously written in terms of phase transition theory, using the order parameter, ϕ. The "chemical reaction" approach is mathematically identical to the phase transition theory approach if the following identifications are made: $G_{\mathrm{A}} \equiv G_0$, $G_{\mathrm{BA}} \equiv -h$, $G_{\mathrm{mix}} \equiv kTf(\phi)$, and $x \equiv \phi$. The condition of chemical reaction equilibrium described above thus results in the explicit relationship between the order parameter of the chemical reaction approach and the ordering field of the chemical reaction approach:

$$h = kT \ln K(p,T) = -G_{\mathrm{BA}}(p,T) = kT \ln \frac{x}{1-x} + \omega(1-2x) \qquad (38)$$

This result shows the explicit relationship between the chemical reaction approach and the phase transition theory approach, allowing me to describe polyamorphism as a generalized "chemical reaction." These approaches are theoretically identical if used in this way. In this formulation of phase transition theory, the general idea of the order parameter and the ordering field is the overall approach, while the "chemical reaction" approach described in this thesis is the specific case of the phase transition theory. Specifically, the theory of phase transitions can essentially be used to describe all kinds of phase transitions, specifically in polyamorphism. The "chemical reaction" approach is unavoidable to describe polyamorphism in a fluid which exhibits a reaction between two species, such as in phosphorus, sulfur, or hydrogen.

However, in all other cases, there must be a way to distinguish between the "chemical reaction" approach and the phase transition theory approach. This must lie in the kinetics of the process, because the thermodynamics of both approaches are similar if not identical. Experiments that detect the vibrational bond differences as well as different dynamic properties of alternative structures in a single component fluid will be able to distinguish the "chemical reaction" approach to modeling polyamorphism as opposed to the approach based on a two scale intermolecular potential. Particularly some of the single component liquids may necessarily require a distinction of states on the molecular level in order to distinguish two distinct states.

A second important question to answer is the interplay of kinetics and thermodynamics. The use of a "chemical reaction" approach necessarily brings up the question of reaction kinetics. Specifically, depending on the reaction kinetics, the fluid may behave as a binary fluid, if the reaction is slow, or as a single component fluid, if the reaction is fast and reaches equilibrium quickly. Whether the fluid must be modeled as a binary mixture or as a single component fluid depends on the separation of time scales: a system with two inter-convertible fluid structures can be thermodynamically treated as a single-component fluid if the time of observation is longer than the characteristic time of "reaction" (fast conversion). In the opposite limit (slow conversion) the system thermodynamically behaves as a two-component mixture. Therefore, in order to apply the "chemical-reaction" approach for the description of fluid polyamorphism I must assume a conversion fast enough to satisfy the equilibrium condition within the observation time scale.

An additional kinetic concern when using the "chemical reaction" approach is the activation energy barrier that arises in all chemical reactions. There are again two important limits that must be considered in order to use the "chemical reaction" approach in the modeling of fluid polyamorphism. In the high activation barrier limit, the amount of energy required to change between two states may be so high that the fluid will not react quickly and therefore must be modeled as a binary fluid. In the low activation barrier limit, the amount of energy required to change between two states will be low enough such that the two alternative structures will have no problem converting between the two energy states and the reaction will reach equilibrium more easily. In order to apply the "chemical reaction" approach here, I must necessarily be in the low activation energy barrier limit.

Also, an important question that the "chemical reaction" approach answers is the number fraction of molecules that are present in one state versus another state when modeling fluid polyamorphism. Some molecular dynamics simulations have been able to define an equilibrium fraction of high density molecules versus low density molecules, but is this a true fraction of molecules present in one state? Could the phase transition approach model the fraction of molecules in each state with the order parameter and the ordering field? Is the chemical reaction approach necessary for the distinguishing of two distinct species in a polyamorphic fluid?

Finally, I have determined a relationship between the energy change between of reaction two states and the temperature of the liquid-liquid critical point. This analysis matches what Stokley et al. [26] previously developed for supercooled water specifically, without referring to a "chemical reaction." Stokley et al.'s language used

a strength of hydrogen bonds that is analogous to the energy change between two states and a strength of hydrogen bond cooperativity as a measure of how non-ideal the system is that is analogous to the position of the liquid-liquid critical point temperature. Figure 38a shows Stokley's figure with the hydrogen bond network language and using the van der Waals equation of state. Figure 38b also shows the work from this Thesis that uses the two structure equation of state described in previous sections.

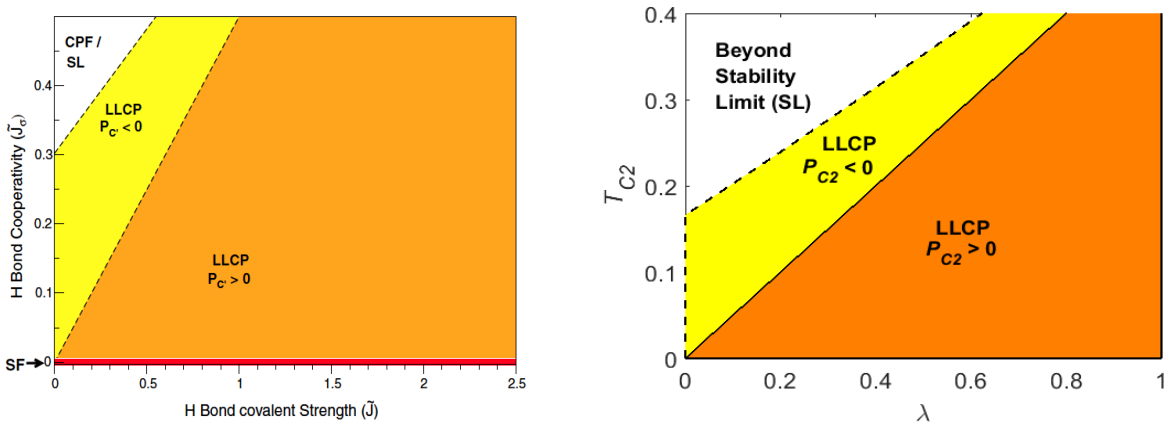

Figure 38. (a) Reproduced from [129]. A plot of hydrogen bond cooperativity versus the hydrogen bond covalent strength. Orange denotes the critical pressure of the liquid-liquid transition is larger than zero. Yellow denotes that the critical pressure is less than zero. White denotes that the critical pressure is below the vapor-liquid spinodal. The red line at cooperativity equals zero is the ideal solution case. (b) Plot comparing λ, the energy change between two states, with the position of the second critical point temperature, a measure of the amount of nonideality in the system. At line T_{c2}=0, the system is completely ideal. The positions of the critical pressures are shown in different colors and with labels.

As stated earlier, the existence of a liquid-liquid separation, in addition to the common gas-liquid transition, in a single-component fluid does not necessarily require the existence of distinct interconvertible molecules or molecular structures. Simulations of molecular models with soft-repulsion intermolecular potentials, such as Jagla model [121, 134, to be published], support this possibility. Moreover, Landau theory of phase transitions can phenomenologically describe this scenario without any reference to interconversion between alternative molecular states.

Let the Gibbs energy of a fluid be described by Eq. (1) with the ordering field $h(p,T)$ in a linearized form as $h = \lambda + \alpha P + \beta T$. The common gas-liquid transition is originated from $G_0(p,T)$. The origin of a possible liquid-liquid transition and the nature of the order parameter depends on a particular form of the function $f(\phi)$. If I adopt a continuous free-energy model for this function, e.g. in the form of the van der Waals Helmholtz energy per unit volume,

$$f(\phi) = \phi \ln \frac{\phi}{1-\phi} - a\phi^2, \qquad (39)$$

(where the interaction parameter a is defined by the second energy scale, while the second distance scale b is incorporated into a and ϕ as $a \to a/b$ and $\phi \to \phi b$) the equilibrium value of the order parameter $\phi_e = \phi(p,T)$ is obtained from

$$h = \frac{\partial f}{\partial \phi} = \frac{kT}{1-\phi} + kT \ln \frac{\phi}{1-\phi} - 2\omega\phi = \lambda + \alpha P + \beta T. \quad (40)$$

Note that in this scenario the order parameter is not an equilibrium fraction of molecules involved in state B because there is no entropy of mixing of two distinct states in the function $f(\phi)$. Instead, the order parameter presumably originates from

two scales in a soft repulsion intermolecular potential, being associated with the excess volume $V_{ex} = V - V_0 = \alpha\phi$ and the excess entropy $S_{ex} = S - S_0 = -\beta\phi$, where $V_0 = \partial G_0 / \partial p$ and $S_0 = -\partial G_0 / \partial T$. The order parameter is zero for a fluid (that is described by a one-scale intermolecular potential) and changing from zero to unity as a function of *p* and *T* for a fluid with a two-scale potential [134, to be published]. Elucidation of the physical nature of the order parameter described by a two scale potential would be a promising project for future studies.

Also note that in the van der Waals–type, continuous scenario of liquid-liquid separation the function $f(\phi)$ is not symmetric with respect to the order parameter. In particular, the critical value of the order parameter $\phi_c = 1/3$ and the critical temperature $T_c = 8a/27k$.

A principal feature of the "chemical reaction" approach is the ability of the model to determine a distinct equilibrium fraction of molecules involved in the low density structure of the liquid. Figure 39 shows the equilibrium fraction of molecules determined by the two structure equation of state described in this thesis, and compares this with the equilibrium fraction of molecules determined by the ST2 model for water [66]. The "chemical reaction" approach qualitatively describes the fraction of molecules in the low density structure similar to what ST2 has calculated.

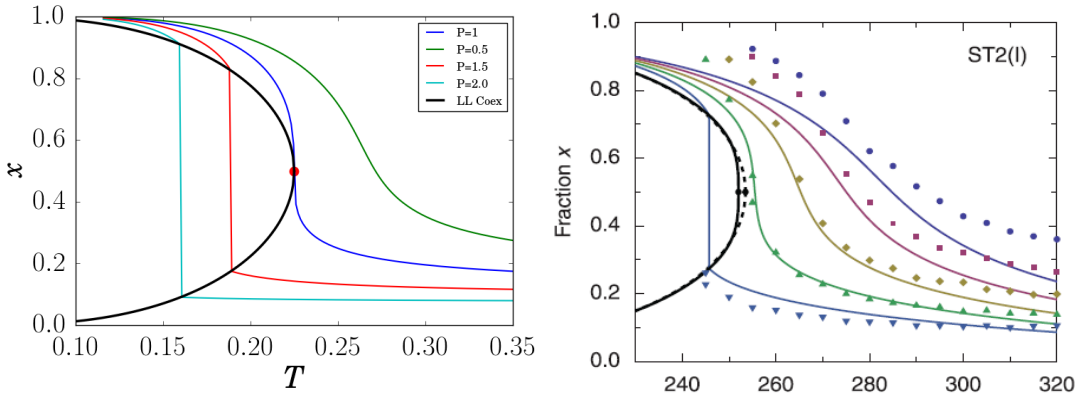

Figure 39. (a) Fraction of state B (low density structure) calculated as a function of temperature along isobars (multicolored lines). Red dot is the liquid-liquid critical point. Black curve is the line of liquid-liquid coexistence. (b) Reproduced from [66]. Fraction of state B (low density structure) calculated as a function of temperature along isobars (multicolored lines). Black curve is the line of liquid-liquid coexistence.

Chapter 5: Conclusion

This Thesis has explored the idea of two structure thermodynamics, from the history of its use, to a new general formulation of a two structure equation of state. By writing an equation of state in terms of Landau phase transition theory, I am able to write a complete general phase transition equation that will work for any microscopic driving force of polyamorphism. I explore the "chemical reaction" approach of modeling polyamorphism, which is a specific case of the general phase transition theory approach. These two approaches can be reconciled and are identical if certain conditions are met.

The "chemical reaction" approach is necessary for substances where polyamorphism is driven by a real chemical reaction (i.e. polymerization in phosphorus, sulfur or hydrogen) or for some generalized "chemical reaction" where two distinct species in a single component fluid can be determined. For the case of supercooled water, there is evidence of two distinct structures of hydrogen bonds that can be determined as two distinct states that can be modeled separately within the two structure equation of state.

The "chemical reaction" approach model qualitatively described the anomalous properties of polyamorphic fluids, including the patterns of extrema lines of density, compressibility and heat capacity. The nonideality of mixing of the two alternative states (that controls the proximity of the liquid-liquid critical point to the liquid-vapor spinodal) is the major factor in determining the shape of the lines of extrema for density, heat capacity and compressibility emanating from the critical point. Additionally, the model is flexible and allows for the investigation of three different scenarios of

polyamorphism. A signature of this model is its ability to describe the order parameter—the existence of the equilibrium fraction of molecules involved in the alternative states in the polyamorphic fluid.

The proximity of the critical point to the limit of absolute stability of the liquid phase is the most important factor in determining the shape of the anomalous density extrema lines. In fact, the density anomaly shrinks and finally disappears at critical points located at negative pressure and directly at or below the limit of absolute stability of the liquid phase. This disappearance of the density anomaly allows me to exclude the possibility of the liquid-liquid critical point in water being located in highly negative pressures or below the limit of stability. This is because the density anomaly is a signature feature of polyamorphic fluids and most simulations and experiments confirm the existence of the density anomaly, even in some specific atomistic models that do not exhibit a liquid-liquid phase transition. Therefore, the density anomaly must be present in order for the critical point to be located at a certain temperature and pressure.

A novel thermodynamic anomaly has been found in the phase diagram of polyamorphic fluids. In the scenario where the critical point is located exactly at the limit of absolute stability, the coexistence is required to reach the critical point from each branch with the same tangent. This results in a bird's beak type of anomaly in this region of the phase diagram.

This work can lead to a variety of future work in the study of polyamorphism. In the future, a more realistic equation of state, such as SAFT, for the vapor-liquid transition (state A in the "chemical reaction" approach) could be used to more

accurately describe a polyamorphic fluid. Polyamorphic fluids often exhibit their transitions at extreme conditions, and modeling these fluids at extreme conditions would be useful. Particularly for the cases of hydrogen and silicon, the modeling of these fluids at extreme conditions could have interesting practical uses. Hydrogen and silicon are both technologically important materials and the knowledge of unusual phase behavior would allow for more novel uses of these fluids. Finally, interesting future work would be the investigation of effects that competing interconvertible states would have on the dynamics of polyamorphic fluids, including the fragile-to-strong transition and the dispersion of sound. These experiments would be able to elucidate the connection between thermodynamics and kinetics.

Appendix A

Calculations for the phase diagrams and lines of extrema were difficult due to the extreme nonlinearity in the equations used for solving. Early iterations of the solutions were solved in Matlab, using numerical solvers built in to the program. After it became clear that the programs in Matlab were not powerful enough to effectively numerically solve the nonlinear equations, due to a large amount of instability. The next iterations of the calculations were completed in Python, but I had very little experience in Python so the calculations were taking a long time. Luckily, with the help of Dr. Michal Duška, who is very skilled in Python, helped me by writing a very powerful code in Python that allowed me to calculate all important information through numerical solvers. Specifically, the code used Brent's method and the bisection method, two rootfinding methods. These methods were useful because the root was found within a range of values specified, ensuring that the correct value was calculated. Brent's method used two different types of extrapolation, either inverse quadratic or hyperbolic, depending on the stability of the solution. Dr. Michal Duška's code allowed me to avoid the instabilities and accurately solve the nonlinear equations.

Appendix B

Table 1. Case numbers and values used for the specific form of ln*K* presented

Case Number	**Λ**	**T_{C2}**	**T_{C2} Values**
A1	0.1	0	0.0001
A2	0.1	$T_{C2}(P_{C2}=1)$	0.025
A3	0.1	$T_{C2}(P_{C2}=P(VL\ coex))$	0.05
A4	0.1	$T_{C2}(P_{C2}<0)$	0.13
A5	0.1	$T_{C2}(P_{C2}=P(spinodal))$	0.202
A6	0,1	$T_{C2}(P_{C2}<P(spinodal))$	0.225
B1	0.5	0	0.0001
B2	0.5	$T_{C2}(P_{C2}=1)$	0.225
B3	0.5	$T_{C2}(P_{C2}=P(VL\ coex))$	0.248
B4	0.5	$T_{C2}(P_{C2}<0)$	0.31
B5	0.5	$T_{C2}(P_{C2}=P(spinodal))$	0.3525
B6	0.5	$T_{C2}(P_{C2}<P(spinodal))$	0.38
C1	1.0	0	0.0001
C2	1.0	$T_{C2}(P_{C2}=1)$	0.475
C3	1.0	$T_{C2}(P_{C2}=P(VL\ coex))$	0.498
C4	1.0	$T_{C2}(P_{C2}<0)$	0.525
C5	1.0	$T_{C2}(P_{C2}=P(spinodal))$	0.549
C6	1.0	$T_{C2}(P_{C2}<P(spinodal))$	0.58

Bibliography

[1] Mitus, A. C., Patashinskii, A. Z., & Shumilo, B. I. The liquid-liquid phase transition. Physics Letters A, 1985, Volume 113, 41-44. doi:10.1016/0375-9601(85)90602-4

[2] Poole, P.H., Grande, T., Angell, C.A., and McMillan, P.F., Polymorphic Phase Transitions in Liquids and Glasses. Science, 1997, Volume 275, 322-323. http://dx.doi.org/10.1126/science.275.5298.322

[3] Tanaka, H. General view of a liquid-liquid phase transition. Physical Review E, 2000, Volume 62, 6968-6976. doi:10.1103/PhysRevE.62.6968

[4] Wilding, M.C., Wilson, M., and McMillan, P.F., Structural studies and polymorphism in amorphous solids and liquids at high pressure. Chemical Society Reviews, 2006, Volume 35, 964–986. http://dx.doi.org/10.1039/b517775h

[5] Ha, A., Cohen, I., Zhao, X.L., Lee, M., and Kivelson, D., Supercooled Liquids and Polyamorphism. The Journal of Physical Chemistry, 1996, Volume 100, 1-4. http://dx.doi.org/10.1021/jp9530820

[6] Cadien, A., Hu, Q.Y., Meng, Y., Cheng, Y.Q., Chen, M.W., Shu, J.F., Mao, H.K., and Sheng, H.W., First-Order Liquid-Liquid Phase Transition in Cerium. Physical Review Letters, 2013, Volume 110, 125503. http://dx.doi.org/10.1103/PhysRevLett.110.125503

[7] Katayama, Y., Mizutani, T., Utsumi, W., Shimomura, O., Yamakata, M., & Funakoshi, K.-i. A first-order liquid-liquid phase transition in phosphorus. Nature, 2000, Volume 403, 170.

[8] Katayama, Y., Mizutani, T., Utsumi, W., Shimomura, O., Yamakata, M., and Funakoshi, K., A first-order liquid-liquid phase transition in phosphorus. Nature, 2000, Volume 403, 170–173. http://dx.doi.org/10.1038/35003143

[9] Katayama, Y., Inamura, Y., Mizutani, T., Yamakata, M., Utsumi, W., & Shimomura, O. Macroscopic separation of dense fluid phase and liquid phase of phosphorus. Science, 2004, Volume 306, 848-851.

[10] Jephcoat, A. P. High-pressure physics: Testing one's metal. Nature materials, 2011 Volume 10, 904-905.

[11] Weir, S.T., Mitchell, A.C., and Nellis, W.J., Metallization of fluid molecular hydrogen at 140 GPa (1.4 Mbar). Physical Review Letters, 1996, Volume 76, 1860-1863. http://dx.doi.org/10.1103/PhysRevLett.76.1860

[12] Dalladay-Simpson, P., Howie, R.T., and Gregoryanz, E., Evidence for a new phase of dense hydrogen above 325 gigapascals. Nature, 2016, Volume 529, 63–67. http://dx.doi.org/10.1038/nature16164

[13] Eremets, M.I., and Troyan, I.A., Conductive dense hydrogen. Nature Materials, 2011, Volume 10, 927-931.http://dx.doi.org/10.1038/NMAT3175

[14] Morales, M.A., Pierleoni, C., Schwegler, E., and Ceperley, D.M., Evidence for a first-order liquid-liquid transition in high-pressure hydrogen from ab initio simulations. Proceedings of the National Academy of Sciences of the United States of America, 2010, Volume 107, 12799-12803. http://dx.doi.org/10.1073/pnas.1007309107

[15] Li, R. Z.; Chen, J.; Li, X. Z.; Wang, E. G.; Xu, L. Supercritical Phenomenon of Hydrogen Beyond the Liquid-Liquid Phase Transition. New J. Phys. 2015, 17, 063023.

[16] Kurita, R., & Tanaka, H. Critical-like Phenomena Associated with Liquid-Liquid Transition in a Molecular Liquid. Science, 2004 Volume 306, 845-848.

[17] Sastry, S., and Angell, C.A., Liquid-liquid phase transition in supercooled silicon. Nature Materials, 2003, Volume 2, 739–743. http://dx.doi.org/10.1038/nmat994

[18] Sciortino F. Liquid-liquid transitions: Silicon in silico. Nature Physics, 2011, Volume 7, 523-524. doi:10.1038/nphys2038

[19] Zhang K., Li H., and Jiang Y.Y., Liquid-liquid phase transition in quasi-two-dimensional supercooled silicon. Physical Chemistry Chemical Physics, 2014, Volume 16, 18023-18028. http://dx.doi.org/10.1039/c4cp00694a

[20] Jakse, N., and Pasturel, A., Liquid-Liquid Phase Transformation in Silicon: Evidence from First-Principles Molecular Dynamics Simulations. Physical Review Letters, 2007, Volume 99, 205702. http://dx.doi.org/10.1103/PhysRevLett.99.205702

[21] Jakse, N., Hennet, L., Price, D.L., Krishnan, S., Key, T., Artacho, E., Glorieux, B., Pasturel, A., and Saboungi, M.L., Structural changes on supercooling liquid silicon. Applied Physics Letters, 2003, Volume 83, 4734-4736. http://dx.doi.org/10.1063/1.1631388

[22] Ganesh, P., and Widom, M., Liquid-Liquid Transition in Supercooled Silicon Determined by First-Principles Simulation. Physical Review Letters, 2009, Volume 102, 075701.http://dx.doi.org/10.1103/PhysRevLett.102.075701

[23] Jakse, N., and Pasturel, A., Dynamic aspects of the liquid-liquid phase transformation in silicon. Journal of Chemical Physics, 2008, Volume 129, 104503 http://dx.doi.org/10.1063/1.2970084

[24] Beye, M., Sorgenfrei, F., Schlotter, W.F., Wurth, W., and Föhlisch, A., The liquid-liquid phase transition in silicon revealed by snapshots of valence electrons. Proceedings of the National Academy of Sciences of the United States of America, 2010, Volume 107, 16772-16776.

[25] Beaucage, P., and Mousseau, N., Liquid–liquid phase transition in Stillinger–Weber silicon. Journal of Physics-Condensed Matter, 2005, Volume 17, 2269–2279. http://dx.doi.org/10.1088/0953-8984/17/15/002

[26] Vasisht, V. V.; Saw, S.; Sastry, S. Liquid-Liquid Critical Point in Supercooled Silicon. Nat. Phys. 2011, 7, 549−553.

[27] Aptekar, L.I., Phase transitions in non-crystalline germanium and silicon. Soviet physics Doklady, 1979, Volume 24, 993–995.

[28] Lacks, D.J., First-order amorphous-amorphous transformation in silica. Physical Review Letters, 2000, Volume 84, 4629–4632. http://dx.doi.org/10.1103/PhysRevLett.84.4629

[29] Shell, M. S.; Debenedetti, P. G.; Panagiotopoulos, A. Z. Molecular Structural Order and Anomalies in Liquid Silica. Phys. Rev. E: Stat. Phys., Plasmas, Fluids, Relat. Interdiscip. Top. 2002, 66, 011202.

[30] Saika-Voivod, I.; Sciortino, F.; Poole, P. H. Computer Simulations of Liquid Silica: Equation of State and Liquid-Liquid Phase Transition. Phys. Rev. E: Stat. Phys., Plasmas, Fluids, Relat. Interdiscip. Top. 2000, 63, 011202.

[31] Lascaris, E. Tunable Liquid-Liquid Critical Point in an Ionic Model of Silica. Phys. Rev. Lett. 2016, 116, 125701.

[32] Lascaris, E.; Hemmati, M.; Buldyrev, S. V.; Stanley, H. E.; Angell, C. A. A. Search for a Liquid-Liquid Critical Point in Models of Silica. J. Chem. Phys. 2014, 140, 224502.

[33] Glosli, J. N.; Ree, F. H. Liquid-Liquid Phase Transformation in Carbon. Phys. Rev. Lett. 1999, 82, 4659−4662.

[34] Greaves, G., Wilding, M.C., Fearn, S., Langstaff, D., Kargl, F., Cox, S., Van, Q.V., Majérus, O., Benmore, C.J., Weber, R., Martin, C.M., and Hennet, L., Detection of First-Order Liquid/Liquid Phase Transitions in Yttrium Oxide-Aluminum Oxide Melts. Science, 2008, Volume 322, 566–570. http://dx.doi.org/10.1126/science.1160766

[35] Barnes, A.C., Skinner, L.B., Salmon, P.S., Bytchkov, A., Pozdnyakova, I., Farmer, T.O., and Fischer, H.E., Liquid/Liquid Phase Transitions in Yttria-Alumina. Physical Review Letters, 2009, Volume 103, 225702. http://dx.doi.org/10.1103/PhysRevLett.103.225702

[36] Angell, C. A. Formation of Glasses from Liquids and Biopolymers. Science, 1995, Volume 267, 1924-1935.

[37] Debenedetti, P. G.; Stillinger, F. H. Supercooled Liquids and the Glass Transition. Nature 2001, 410, 259−267.

[38] Sastry, S. Supercooled Water: Going Strong or Falling Apart?. Nature, 1999 Volume 398, 467-469 doi:10.1038/18982

[39] Sun, Q.; Zhou, C.; Yue, Y.; Hu, L. A Direct Link Between the Fragile-to-Strong Transition and Relaxation in Supercooled Liquids. J. Phys. Chem. Lett. 2014, 5, 1170−1174.

[40] Ito, K.; Moynihan, C. T.; Angell, C. A. Thermodynamic Determination of Fragility in Liquids and a Fragile-to-Strong Liquid Transition in Water. Nature 1999, 398, 492−495.
[41] Debenedetti, P. G. Supercooled and Glassy Water. J. Phys.: Condens. Matter 2003, 15, R1669−R1726.
[42] Debenedetti, P. G.; Stanley, H. E. Supercooled and Glassy Water. Phys. Today 2003, 56, 40−46.
[43] Speedy, R. J.; Angell, C. A. Isothermal Compressibility of Supercooled Water and Evidence for a Thermodynamic Singularity at−45°C. J. Chem. Phys. 1976, 65, 851−858.
[44] Kumar, P.; Stanley, H. E. Thermal Conductivity Minimum: A New Water Anomaly. J. Phys. Chem. B 2011, 115, 14269−14273.
[45] Angell, C. A.; Oguni, M.; Sichina, W. J. Heat Capacity of Water at Extremes of Supercooling and Superheating. J. Phys. Chem. 1982, 86,998−1002.
[46] Kanno, H.; Angell, C. A. Water: Anomalous Compressibilities to1.9 kbar and Correlation with Supercooling Limits. J. Chem. Phys. 1979, 70, 4008−4016.
[47] Vega, C.; Abascal, J. L. F. Relation Between the Melting Temperature and the Temperature of Maximum Density for the Most Common Models of Water. J. Chem. Phys. 2005, 123, 144504.
[48] Gallo, P., Arnann-Winkel, K., Angell, C.A., Anisimov, M.A., Caupin, F., Chakravarty, C., Lascaris, E., Loerting, T., Panagiotopoulos, A.Z., Russo, J., Sellberg, J.A., Stanley, H.E., Tanaka, H., Vega, C., Xu, L.M., and Pettersson, L.G.M., Water: A Tale of Two Liquids. Chemical Reviews, 2016, Volume116, 7463-7500. http://dx.doi.org/10.1021/acs.chemrev.5b00750
[49] Poole, P.H., Sciortino, F., Essman, U., and Stanley, H.E., Phase behavior of metastable water. Nature, 1992, Volume 360, 324-328. http://dx.doi.org/10.1038/360324a0
[50] Hare, D. E.; Sorensen, C. M. The Density of Supercooled Water. II. Bulk Samples Cooled to the Homogeneous Nucleation Limit. J. Chem. Phys. 1987, 87, 4840−4845.
[51] Abascal, J. L. F.; Vega, C. A General Purpose Model for the Condensed Phases of Water. J. Chem. Phys. 2005, 123, 234505.
[52] Sastry, S.; Debenedetti, P. G.; Sciortino, F.; Stanley, H. E. Singularity-Free Interpretation of the Thermodynamics of Supercooled Water. Phys. Rev. E: Stat. Phys., Plasmas, Fluids, Relat. Interdiscip. Top.1996, 53, 6144−6154.
[53] Speedy, R. J. Stability-Limit Conjecture. J. Phys. Chem. 1982, 86, 982−989.
[54] Tanaka, H. Simple Physical Model of Liquid Water. J. Chem. Phys.2000, 112, 799−809.
[55] Fuentevilla, D. A.; Anisimov, M. A. Scaled Equation of State for Supercooled Water Near the Liquid-Liquid Critical Point. Phys. Rev. Lett. 2006, 97, 195702.

[56] Bertrand, C. E.; Anisimov, M. A. Peculiar Thermodynamics of the Second Critical Point in Supercooled Water. J. Phys. Chem. B 2011, 115,14099−14111.

[57] Poole, P. H.; Sciortino, F.; Essmann, U.; Stanley, H. E. The Spinodal of Liquid Water. Phys. Rev. E: Stat. Phys., Plasmas, Fluids, Relat. Interdiscip. Top. 1993, 48, 3799−3817.

[58] Sciortino, F.; Poole, P. H.; Essmann, U.; Stanley, H. E. Line of Compressibility Maxima in the Phase Diagram of Supercooled Water. Phys. Rev. E: Stat. Phys., Plasmas, Fluids, Relat. Interdiscip. Top. 1997, 55,727−737.

[59] Franzese, G., Malescio, G., Skibinsky, A., Buldyrev, S.V., and Stanley, H.E., Generic mechanism for generating a liquid–liquid phase transition. Nature, 2001, Volume 409, 692-695. http://dx.doi.org/10.1038/35055514

[60] Palmer, J.C., Martelli, F., Liu, Y., Car, R., Panagiotopoulos, A.Z., and Debenedetti, P.G., Metastable liquid-liquid transition in a molecular model of water. Nature, 2014, Volume 510, 385–388. http://dx.doi.org/10.1038/nature13405

[61] Xu, L., Kumar, P., Buldyrev, S.V., Chen, S.H., Poole, P.H., Sciortino, F., and Stanley, H.E., Relation between the Widom line and the dynamic crossover in systems with a liquid-liquid critical point. Proceedings of the National Academy of Sciences of the United States of America, 2005, Volume102, 16558-16562. http://dx.doi.org/10.1073/pnas.0507870102

[62] Mishima, O.; Stanley, H. E. The Relationship Between Liquid, Supercooled and Glassy Water. Nature 1998, 396, 329−335.

[63] Stanley, H. E.; Kumar, P.; Franzese, G.; Xu, L.; Yan, Z.; Mazza, M.G.; Buldyrev, S. V.; Chen, S.-H.; Mallamace, F. Liquid Polyamorphism: Possible Relation to the Anomalous Behavior of Water. Eur. Phys. J.: Spec. Top. 2008, 161, 1−17.

[64] Smith, R. S.; Kay, B. D. The Existence of Supercooled Liquid Water at 150 K. Nature 1999, 398, 788−791.

[65] Holten, V.; Anisimov, M. A. Entropy-Driven Liquid-Liquid Separation in Supercooled Water. Sci. Rep. 2012, 2, 713.

[66] Holten V, Palmer JC, Poole PH, Debenedetti PG, & Anisimov MA. Two-state thermodynamics of the ST2 model for supercooled water. The Journal Of Chemical Physics, 2014, Volume 140, 104502. doi:10.1063/1.4867287

[67] Peter H Poole, Ivan Saika-Voivod, & Francesco Sciortino. Density minimum and liquid-liquid phase transition. Journal Of Physics: Condensed Matter, 2005, Volume 17, L431-L437. doi:10.1088/0953-8984/17/43/L01

[68] Holten V, Limmer DT, Molinero V, & Anisimov MA. Nature of the anomalies in the supercooled liquid state of the mW model of water. The Journal Of Chemical Physics, 2013, Volume 138, 174501. doi:10.1063/1.4802992

[69] Singh, R. S., Biddle, J. W., Debenedetti, P. G., & Anisimov, M. A. Two-state thermodynamics and the possibility of a liquid-liquid phase transition in supercooled

TIP4P/2005 water. The Journal Of Chemical Physics, 2016, Volume 144(14), 144504. doi:10.1063/1.4944986

[70] Abascal, J. L. F.; Vega, C. Widom Line and the Liquid-Liquid Critical Point for the TIP4P/2005 Water Model. J. Chem. Phys. 2010,133, 234502.

[71] González MA, Valeriani C, Caupin F, & Abascal JL. A comprehensive scenario of the thermodynamic anomalies of water using the TIP4P/2005 model. The Journal Of Chemical Physics, 2016, Volume 14, 054505. doi:10.1063/1.4960185

[72] Biddle, J. W., Singh, R. S., Sparano, E. M., Ricci, F., González, M. A., Valeriani, C., ... Caupin, F. Two-structure thermodynamics for the TIP4P/2005 model of water covering supercooled and deeply stretched regions. The Journal Of Chemical Physics, 2017, Volume 146, 034502. doi:10.1063/1.4973546

[73] Brovchenko, I.; Geiger, A.; Oleinikova, A. Multiple Liquid-Liquid Transitions in Supercooled Water. J. Chem. Phys. 2003, 118, 9473−9476.

[74] Brovchenko, I.; Geiger, A.; Oleinikova, A. Liquid-Liquid Phase Transitions in Supercooled Water Studied by Computer Simulations of Various Water Models. J. Chem. Phys. 2005, 123, 044515.

[75] Jedlovszky, P.; Vallauri, R. Liquid-Vapor and Liquid-Liquid Phase Equilibria of the Brodholt-Sampol-Vallauri Polarizable Water Model. J. Chem. Phys. 2005, 122, 081101.

[76] Buldyrev, S. V.; Stanley, H. E. A System with Multiple Liquid-Liquid Critical Points. Phys. A 2003, 330, 124−129.

[77] Liu, Y.; Panagiotopoulos, A. Z.; Debenedetti, P. G. Low-Temperature Fluid-Phase Behavior of ST2 Water. J. Chem. Phys. 2009,131, 104508.

[78] Xu, L.; Buldyrev, S. V.; Giovambattista, N.; Angell, C. A.; Stanley,H. E. A Monatomic System with a Liquid-Liquid Critical Point and Two Distinct Glassy States. J. Chem. Phys. 2009, 130, 054505.

[79] Xu, L.; Giovambattista, N.; Buldyrev, S. V.; Debenedetti, P. G.;Stanley, H. E. Waterlike Glass Polyamorphism in a Monoatomic Isotropic Jagla Model. J. Chem. Phys. 2011, 134, 064507.

[80] Liu, Y.; Palmer, J. C.; Panagiotopoulos, A. Z.; Debenedetti, P. G. Liquid-Liquid Transition in ST2 Water. J. Chem. Phys. 2012, 137,214505.

[81] Liu, Y.; Panagiotopoulos, A. Z.; Debenedetti, P. G. Low-Temperature Fluid-Phase Behavior of ST2 Water. J. Chem. Phys. 2009,131, 104508.

[82] Palmer, J. C.; Martelli, F.; Liu, Y.; Car, R.; Panagiotopoulos, A.Z.; Debenedetti, P. G. Metastable Liquid-Liquid Transition in a Molecular Model of Water. Nature 2014, 510, 385−388.

[83] Harrington, S.; Poole, P. H.; Sciortino, F.; Stanley, H. E. Equation of State of Supercooled Water Simulated using the Extended Simple Point Charge Intermolecular Potential. J. Chem. Phys. 1997, 107,7443−7450.

[84] Li, Y.; Li, J.; Wang, F. Liquid-Liquid Transition in Supercooled Water Suggested by Microsecond Simulations. Proc. Natl. Acad. Sci. U. S.A. 2013, 110, 12209−12212.

[85] Holten V, Bertrand CE, Anisimov MA, & Sengers JV. Thermodynamics of supercooled water. The Journal Of Chemical Physics, 2012, Volume 136, 094507. doi:10.1063/1.3690497

[86] Whiting, H. A New Theory of Cohesion Applied to the Thermodynamics of Liquids and Solids. Proc. Am. Acad. Arts Sci. 1883, Volume 19, 353−431.

[87] Röntgen, W. K. Ueber die Constitution des Flüssigen Wassers. Ann. Phys. 1892, 281, 91−97.

[88] Limmer, D. T.; Chandler, D. Time Scales of Supercooled Water and Implications for Reversible Polyamorphism. Mol. Phys. 2015, 113,2799−2804.

[89] Errington, J. R.; Debenedetti, P. G. Relationship Between Structural Order and the Anomalies of Liquid Water. Nature 2001, 409,318−321.

[90] Russo, J.; Tanaka, H. Understanding Water's Anomalies with Locally Favoured Structures. Nat. Commun. 2014, 5, 3556.

[91] Rapoport, E., Model for melting curve maxima at high pressure. Journal of Chemical Physics, 1967, Volume 46, 2891-2895. http://dx.doi.org/10.1063/1.1841150

[92] Moynihan, C.T., Two species nonideal solution model for amorphous amorphous phase transitions. Materials Research Society Conference Proceedings, 1997, Volume 455, 411–425.

[93] Jeffery, C. A.; Austin, P. H. A New Analytic Equation of State for Liquid Water. J. Chem. Phys. 1999, 110, 484−496.

[94] Kiselev, S. B. Physical Limit of Stability in Supercooled Liquids. Int. J. Thermophys. 2001, 22, 1421−1433.

[95] Cuthbertson, M. J.; Poole, P. H. Mixturelike Behavior Near a Liquid-Liquid Phase Transition in Simulations of Supercooled Water. Phys. Rev. Lett. 2011, 106, 115706.

[96] Moore, E. B.; Molinero, V. Structural Transformation in Supercooled Water Controls the Crystallization Rate of Ice. Nature2011, 479, 506−508.

[97] Taschin A, Bartolini P, Eramo R, Righini R, & Torre R. Evidence of two distinct local structures of water from ambient to supercooled conditions. Nature Communications, 2013, Volume 4, 2401. doi:10.1038/ncomms3401

[98] Sellberg JA, Huang C, McQueen TA, Loh ND, Laksmono H, Schlesinger D, ... Nilsson A. Ultrafast X-ray probing of water structure below the homogeneous ice nucleation temperature. Nature, 2014, Volume 510, 381-4. doi:10.1038/nature13266

[99] Tokushima, T.; Harada, Y.; Takahashi, O.; Senba, Y.; Ohashi, H.; Pettersson, L. G. M.; Nilsson, A.; Shin, S. High Resolution X-ray Emission Spectroscopy of

Liquid Water: The Observation of Two Structural Motifs. Chem. Phys. Lett. 2008, 460, 387−400.

[100] Tokushima, T.; Harada, Y.; Horikawa, Y.; Takahashi, O.; Senba, Y.; Ohashi, H.; Pettersson, L. G. M.; Nilsson, A.; Shin, S. High Resolution X-ray Emission Spectroscopy of Water and Its Assignment Based on Two Structural Motifs. J. Electron Spectrosc. Relat. Phenom.2010, 177, 192−205.

[101] Soper, A. K.; Teixeira, J.; Head-Gordon, T. Is Ambient Water Inhomogeneous on the Nanometer-Length Scale? Proc. Natl. Acad. Sci.U. S. A. 2010, 107, E44.

[102] Myneni, S.; Luo, Y.; Näslund, L.-Å.; Cavalleri, M.; Ojamäe, L.;Ogasawara, H.; Pelmenschikov, A.; Wernet, P.; Väterlein, P.; Heske, C.;Hussain, Z.; Pettersson, L. G. M.; Nilsson, A. Spectroscopic Probing of Local Hydrogen Bonding Structures in Liquid Water. J. Phys.: Condens. Matter 2002, 14, L213−L219.

[103] Nilsson, A.; Nordlund, D.; Waluyo, I.; Huang, N.; Ogasawara,H.; Kaya, S. H.; Bergmann, U.; Näslund, L.-Å.; Öström, H.; Wernet, P.;Andersson, K.; Schiros, T.; Pettersson, L. G. M. X-ray Absorption Spectroscopy and X-ray Raman Scattering of Water: An Experimental View. J. Electron Spectrosc. Relat. Phenom. 2010, 177, 99−129.

[104] Chen, W.; Wu, X.; Car, R. X-ray Absorption Signatures of the Molecular Environment in Water and Ice. Phys. Rev. Lett. 2010, 105,017802.

[105] Pettersson, L. G. M.; Nilsson, A. The Structure of Water from Ambient to Deeply Supercooled. J. Non-Cryst. Solids 2015, 407, 399−417.

[106] Fuchs, O.; Zharnikov, M.; Weinhardt, L.; Blum, M.; Weigand,M.; Zubavichus, Y.; Bär, M.; Maier, F.; Denlinger, J. D.; Heske, C.;Grunze, M.; Umbach, E. Isotope and Temperature Effects in Liquid Water Probed by X-ray Absorption and Resonant X-ray Emission Spectroscopy. Phys. Rev. Lett. 2008, 100, 027801.

[107] Nilsson, A.; Tokushima, T.; Horikawa, Y.; Harada, Y.;Ljungberg, M. P.; Shin, S.; Pettersson, L. G. M. Resonant Inelastic Xray Scattering of Water. J. Electron Spectrosc. Relat. Phenom. 2013, 188,84−100.

[108] Nilsson, A.; Pettersson, L. G. M. The Structural Origin of Anomalous Properties of Liquid Water. Nat. Commun. 2015, 6, 8998.

[109] Sciortino, F.; La Nave, E.; Tartaglia, P. Physics of the Liquid-Liquid Critical Point. Phys. Rev. Lett. 2003, 91, 155701.

[110] Bellissent-Funel, M.-C.; Bove, L.; Nilsson, A.; Paciaroni, A.; Schlesinger, D.; Skinner, L.; Amann-Winkel, K. X-ray and Neutron Scattering of Water. Chem. Rev. 2016, 106, 10.1021/acs.chemrev.5b00663.

[111] Davis, J.; C, M.; Litovitz, T. A. Two-State Theory of the Structure of Water. J. Chem. Phys. 1965, 42, 2563−2576.

[112] Vedamuthu, M.; Singh, S.; Robinson, G. W. Properties of Liquid Water: Origin of the Density Anomalies. J. Phys. Chem. 1994, 98, 2222−2230.

[113] Soper, A. K.; Ricci, M. A. Structures of High-Density and Low-Density Water. Phys. Rev. Lett. 2000, 84, 2881−2884.
[114] Bellissent-Funel, M. C. Is there a Liquid-Liquid Phase Transition in Supercooled Water? Europhys. Lett. 1998, 42, 161−166.
[115] Mishima, O. Volume of Supercooled Water under Pressure and the Liquid-Liquid Critical Point. J. Chem. Phys. 2010, 133, 144503.
[116] Stillinger, F. H.; Rahman, A. Improved Simulation of Liquid Water by Molecular Dynamics. J. Chem. Phys. 1974, 60, 1545−1557.
[117] Yagasaki, T.; Matsumoto, M.; Tanaka, H. Spontaneous Liquid-Liquid Phase Separation of Water. Phys. Rev. E 2014, 89, 020301.
[118] Smallenburg, F.; Sciortino, F. Tuning the Liquid-Liquid Transition by Modulating the Hydrogen-Bond Angular Flexibility in a Model for Water. Phys. Rev. Lett. 2015, 115, 015701.
[119] Tanaka, H. Thermodynamic Anomaly and Polyamorphism of Water. Europhys. Lett. 2000, 50, 340−346.
[120] Buldyrev, S. V., Malescio, G., Angell, C. A., Giovambattista, N., Prestipino, S., Saija, F, ... Xu, L. Unusual phase behavior of one-component systems with two-scale isotropic interactions. Journal Of Physics: Condensed Matter, 2009, Volume 21 doi:10.1088/0953-8984/21/50/504106
[121] Jagla, E. A. Core-Softened Potentials and the Anomalous Properties of Water. J. Chem. Phys. 1999, 111, 8980−8986.
[122] Xu, L.; Buldyrev, S. V.; Angell, C. A.; Stanley, H. E. Thermodynamics and Dynamics of the Two-Scale Spherically Symmetric Jagla Ramp Model of Anomalous Liquids. Phys. Rev. E2006, 74, 031108.
[123] Xu, L.; Ehrenberg, I.; Buldyrev, S. V.; Stanley, H. E. Relationship Between the Liquid- Liquid Phase Transition and Dynamic Behavior in the Jagla Model. J. Phys.: Condens. Matter 2006, 18, S2239−S2246.
[124] Franzese, G.; Malescio, G.; Skibinsky, A.; Buldyrev, S. V.; Stanley, H. E. Generic Mechanism for Generating a Liquid-Liquid Phase Transition. Nature 2001, 409, 692−695.
[125] Tu, Y.; Buldyrev, S. V.; Liu, Z.; Fang, H.; Stanley, H. E. Different Water Scenarios for a Primitive Model with Two Types of Hydrogen Bonds. Europhys. Lett. 2012, 97, 56005.
[126] Ponyatovsky, E. G.; Sinitsyn, V. V.; Pozdnyakova, T. A. The Metastable T-P Phase Diagram and Anomalous Thermodynamic Properties of Supercooled Water. J. Chem. Phys. 1998, 109, 2413−2422.
[127] Holten, V.; Sengers, J. V.; Anisimov, M. A. Equation of State for Supercooled Water at Pressures up to 400 MPa. J. Phys. Chem. Ref. Data2014, 43, 043101.

[128] Smallenburg, F.; Filion, L.; Sciortino, F. Erasing No-Man's Land by Thermodynamically Stabilizing the Liquid-Liquid Transition in Tetrahedral Particles. Nat. Phys. 2014, 10, 653−657.
[129] Stokely K, Mazza MG, Stanley HE, & Franzese G. Effect of hydrogen bond cooperativity on the behavior of water. Proceedings Of The National Academy Of Sciences Of The United States Of America, 2010, Volume 107, 1301-6. doi:10.1073/pnas.0912756107
[130] Ciach A, Góźdź W, & Perera A. Simple three-state lattice model for liquid water. Physical Review. E, Statistical, Nonlinear, And Soft Matter Physics, 2008, Volume 78, 021203.
[131] Poole, P. H., Sciortino, F., Grande, T., Stanley, H. E., & Angell, C. A. Effect of Hydrogen Bonds on the Thermodynamic Behavior of Liquid Water. Physical Review Letters, 1994, Volume 73, 1632-1635. doi:10.1103/PhysRevLett.73.1632
[132] Landau, L.D. and Lifshitz, E.M., Statistical Physics, Pergamon Press, 1980
[133] Frenkel, J., Kinetic Theory of Liquids, Dover Publications, 1946
[134] Ricci, F. and Debenedetti, P. G., A Free Energy Study of the Liquid-Liquid Phase Transition of the Jagla Two-Scale Potential. 2017, to be published

List of Presentations and Publications

Presentations

Lauren E. Amrhein and Mikhail A. Anisimov. : Liquid polyamorphism: Equation of state of a fluid with thermodynamic equilibrium between two structures. US-Russia Workshop on Phase Transitions in Fluids and Plasmas (College Park, MD). 2016
Speaker: Lauren E. Amrhein

Lauren E. Amrhein, Amanda Rosenbaum, Frédéric Caupin and Mikhail A. Anisimov. Thermodynamics of Liquid Polyamorphism: Equation of State of a Fluid with Thermodynamic Equilibrium Between Two Structures. National American Institute of Chemical Engineers (AIChE) Conference (San Francisco, CA). 2016.
Speaker: Lauren E. Amrhein

Lauren Amrhein, Frédéric Caupin, Michal Duŝka, Amanda Rozenbaum, Richard Sadus, and Mikhail A. Anisimov. Fluid polyamorphism induced by chemical reaction equilibrium. 2nd US-Russia Workshop on Phase Transitions in Fluids and Plasmas (College Park, MD). 2017.

Submitted- Lauren Amrhein, Mikhail A. Anisimov, Frédéric Caupin, Michal Duŝka, and Amanda Rosenbaum. Thermodynamics of Fluid Polyamorphism. National American Institute of Chemical Engineers (AIChE) Conference (Minneapolis, MN) 2017.
Speaker: Lauren E. Amrhein

Publications

To be submitted- Lauren Amrhein, Mikhail A. Anisimov, Frédéric Caupin, Michal Duŝka, and Amanda Rosenbaum. Thermodynamics of Fluid Polyamorphism. Proceedings of the National Academy of Sciences. 2017